β-catenin perturbations control differentiation programs in mouse embryonic stem cells

Elisa Pedone[1,2,+], Mario Failli[3], Gennaro Gambardella[3], Rossella De Cegli[3], Diego di Bernardo[3,4] and Lucia Marucci[1,2,5,+].

[1]Department of Engineering Mathematics, University of Bristol, Bristol BS8 1UB, UK. [2]School of Cellular and Molecular Medicine, University of Bristol, Bristol BS8 1TD, UK. [3]Telethon Institute of Genetic and Medicine Via Campi Flegrei 34, 80078 Pozzuoli, Italy.[4]Department of Chemical, Materials and Industrial Production Engineering, University of Naples Federico II, 80125 Naples, Italy. [5]BrisSynBio, Bristol BS8 1TQ, UK.

[+] corresponding authors; elisa.pedone@bristol,ac,uk; lucia.marucci@bristol.ac.uk

Abstract

The Wnt/β-catenin pathway is involved in development, cancer and embryonic stem cell (ESC) maintenance; its dual role in stem cell self-renewal and differentiation is still controversial. Here, we applied an elegant *in vitro* system enabling conditional β-catenin control in β-catenin null mouse ESCs. We report that moderate activation of the canonical Wnt pathway via β-catenin genetic manipulation enhances epiblast stem cell (EpiSC) derivation *in vitro*. Using a different genetic model and β-catenin chemical modulation, we derive a new protocol for ESCs to EpiSCs differentiation, based on NDfi227 and the GSK3α/β inhibitor Chiron, that is more efficient than standard FGF2/ActivinA-based protocols. Finally, we report that moderate β-catenin favours early stem cell commitment towards mesoderm if overexpressed in the 'ground state' of pluripotency only, or endoderm if the overexpression is maintained also during the differentiation, unravelling the controversial role of this signalling pathway at the exit from pluripotency.

Introduction

Pluripotent Cells (PCs) are characterized by indefinite proliferative and differentiation potential and their identity is determined by the balance between signals promoting self-renewal and differentiation. The first step for stem cells differentiation is the exit from the pluripotent state, tightly controlled by underlying gene regulatory network dynamics which can drive specific lineage commitment. During murine development *in vivo*, embryonic stem cells (ESCs), that represent the naïve pluripotent state of the early epiblast[1-3], convert into the late epiblast and finally in terminally differentiated

somatic cells. ESCs can be derived from the pre-implantation epiblast and used to study cell pluripotency and differentiation, proving an excellent *in vitro* system for understanding signalling pathways interplay in this transition. In serum-based cultures, mouse ESCs (hereafter called ESCs) are heterogeneous for the expression of pluripotency genes[1,2,4-10], while, when cultured in serum-free media supplemented with inhibitors of MEK1/2 (PD) and GSK3α/β (Chiron) in the presence or not of the Leukaemia Inhibitory Factor-LIF (2i or 2i+LIF)[3], a uniform self-renewal condition known as 'ground state of pluripotency', characterized by homogenous gene expression[11-14], genome demethylation[15-17] and stable naive pluripotency[18,19], is established.

Mouse epiblast stem cells (hereafter called EpiSCs) also represent a relevant *in vitro* model because of their similarities with embryonic stem cells of human origin[20]. EpiSCs, derived from the post-implantation epiblast, are also capable of differentiating in all the germ-layers[20,21], however, they differ from ESCs in shape, clonogenicity, gene expression, epigenome status and, most importantly, contribution to chimaeras[14,20-22]. EpiSCs require ActivinA and the fibroblast growth factor 2 (FGF2)[20,21] for *in vitro* expansion; of note, FGF signalling pathway activation, while promoting EpiSC self-renewal, induces ESC differentiation[23,24]. FGF2 treatment, in combination or not with Activin and LIF/STAT3 pathway inhibitors, has been used for ESCs differentiation into EpiSCs both in serum-based and serum-free culture conditions[25-28], although with low efficiency. Self-renewing EpiSCs have been recently established by simultaneous activation and inhibition of the Wnt/β-catenin pathway[29]; however, the effect of these perturbations on ESCs-EpiSCs direct transition has not been explored.

The Wnt/β-catenin is a highly conserved signalling pathway involved in ESCs self-renewal[30] and cell-cycle progression[31]. β-catenin levels are tightly controlled by the active transcription of negative regulators working at different levels of the signalling cascade[32]: Axin2[33-35] is part of the disruption complex whereas DKK1[36] binds the Wnt receptor complex attenuating cellular response; these negative feedback loops contribute to the emergence of nonlinear dynamics in the Wnt/β-catenin pathway, proved to be important in different biological and developmental aspects (reviewed in[37]), ESCs pluripotency[10] and somatic cell reprogramming[10,38-41]. The role of the canonical Wnt pathway in early *in vivo* developmental stages and the requirement of

its activation for ESCs self-renewal have been a matter of intense research, often generating contradictory results[3,42-47]. Pluripotency incompetence has been reported in two independent studies using β-catenin$^{-/-}$ ECSs[42,44]; this phenotype was, however, contradicted in later studies with newly generated β-catenin$^{-/-}$ cell lines, which normally self-renew in both serum- and 2i-LIF but fail to differentiate when LIF-deprived[45-47]. Such knock-out models provided an excellent *in vitro* system to study β-catenin function on cell-decision making in a β-catenin null background.

Here, we take advantage of the β-catenin$^{-/-}$ ESC line generated by Aulicino and colleagues[45], where the entire β-catenin coding sequence was removed to avoid possible compensatory mechanisms from aberrant truncated isoforms, to study the effect of dose and time-varying β-catenin modulation on the exit from pluripotency and differentiation. Increasing β-catenin doses have been indirectly achieved in the past by mutating the adenomatous polyposis coli gene (APC)[48]; teratomas from the mutants with the highest β-catenin transcriptional activity showed major differentiation defects in the neuroectoderm, dorsal mesoderm and endoderm. However, it is important to notice that mutants with β-catenin accumulation but reduced nuclear translocation normally contribute to all the germ layers[48], suggesting that other mechanisms, β-catenin dependent or independent (e.g., active nuclear translocation), might be involved in differentiation impairment. Therefore, cellular models enabling modulation of β-catenin itself are necessary to systematically associate protein perturbations to pluripotency and differentiation phenotypes.

We tuned β-catenin levels in β-catenin$^{-/-}$ ESCs applying an improved inducible system[49] and measured both the global gene expression following 2i/LIF withdrawal, and the efficiency of ESC-EpiSC transition *in vitro*. Comparing the response to differentiation stimuli of ESCs expanded in serum/LIF or 2i/LIF, we demonstrated that moderate β-catenin overexpression in β-catenin$^{-/-}$ ESCs enhances the differentiation efficiency into EpiSCs. Moreover, short-term expansion in 2i/LIF predisposes ESCs to such transition, challenging the hypothesis of a synergistic effect of the ERK, Wnt/β-catenin and STAT pathways on EpiSCs derivation *in vitro* that would require further investigation. These results were recapitulated by exposing wild-type ESCs to low doses of the GSK3α/β inhibitor Chiron, further confirming our findings and providing an improved protocol for fast and efficient *in vitro* derivation of EpiSCs. Finally, the transcriptome of ESCs expressing different β-catenin levels confirmed what we and

others reported about β-catenin dispensable requirement for pluripotency establishment[45-47,49], while suggesting that specific β-catenin perturbations establish a bias towards the endoderm lineage.

Overall, our study highlights that synergistic effects of β-catenin doses and culture conditions control *in vitro* ESC fate decision-making.

Results

Wnt/β-catenin pathway perturbations control *in vitro* generation of EpiSC

To study the role of the Wnt/β-catenin pathway in EpiSC derivation *in vitro*, we used the C1-EF1a-rtTA_TRE3G-DDmCherryβ-catenin^{S33Y} (hereafter called C1) ESC line we previously generated[49]. Briefly, β-catenin$^{-/-}$ ESCs[45] were modified to stably express a doxycycline-inducible fusion protein comprising the conditional destabilising domain (DD), the mCherry fluorescent protein and the constitutive active β-catenin^{S33Y}(Figure 1A)[50]. The inducer molecule doxycycline (Doxy) enables transcriptional initiation, while trimethoprim (TMP) allows protein stabilisation by inactivating the DD (Figure 1A)[49]. The use of a constitutively active and tunable β-catenin^{S33Y} form, uncoupled from upstream endogenous regulations and in a knock-out background, would help in dissecting β-catenin functions in the ESCs-EpiSCs transition, avoiding compensatory mechanisms and possible off-target effects of chemical compounds.

We confirmed, in C1 cells, the correct induction (Figure 1A, inset and[49]), intracellular distribution and functionality of the exogenous protein following input administration[49]. We previously confirmed the dispensable role of β-catenin in pluripotent culture conditions and showed that moderate β-catenin overexpression (i.e., TMP10μM_Doxy10ng/mL) can protect cells from exiting pluripotency in the absence of both serum and LIF[49]. Following these results, we measured the efficiency of EpiSCs derivation when overexpressing different amounts of exogenous β-catenin in pluripotent conditions and/or during differentiation, adapting existing differentiation protocols[29,51] (see Methods for details). To observe how the cellular response changes depending on the culture condition, C1 ESCs were expanded either in serum/LIF (hereafter called FBS/L) and 2iLIF (hereafter called 2i/L). ESCs in 'ground state' media (i.e., cultured in 2i/L)[3] have been extensively characterised for their transcriptional and epigenetic homogeneity[12,14] and resemblance of the pre-

implantation epiblast[11,15-18]. However, prolonged culture in 2i/L results in epigenetic changes impairing normal differentiation *in vitro* and development *in vivo*[52]. Therefore, we opted for a short-term culture in 2i/L (3 passages), sufficient to obtain cell homogeneity while avoiding possible aberrations.

ESCs from FBS/L or 2i/L (Figure 1B, C) were cultured for 48 hrs either in DMSO (Figure 1B) or in presence of maximum TMP (10μM) combined with low (10ng/mL) or saturating (100ng/mL) Doxy (Figure 1C). The concentrations of Doxy were extrapolated from flow cytometry measurements of the mCherry signal to provide two levels (moderate and high) of exogenous protein (Figure 1A, inset). We next seeded 1.5×10^4 cells/cm^2 on a fibronectin-coated plate in NDiff227[26] supplemented with ActivinA, FGF2[29] and different combinations of DMSO, TMP and Doxy (Figure 1B, C and Methods). Cells kept under these conditions for 4 days, with media refreshed after the first 2 culture days, were subsequently analysed for the expression of the Epiblast marker Fgf5 by qPCR (Figure 1B, C).

TMP/Doxy pre-treatment before differentiation (Figure 1C) did not alter the basal Fgf5 expression of FBS/L ESCs (T0 samples in Figure 1D), whereas that of TMP10μM_Doxy10ng/mL treated ESCs from 2i/L culture was higher compared to the TMP10μM_Doxy100ng/mL and the TMP10μM treated samples (T0 samples in Figure 1E).

In all Doxy/TMP treated conditions, Fgf5 levels were higher when C1 ESCs were pre-cultured in 2i/L, suggesting that the latter predisposes cells to more efficiently differentiate into EpiSCs (Figure 1E). In both scenarios (i.e., from FBS/L or 2i/L), β-catenin overexpression in pluripotent conditions only (i.e., “Before” in Figure 1D, E), or both before and during differentiation (i.e., “Always” in Figure 1D, E), did not increase Fgf5 levels as compared to TMP10μM-treated C1 ESCs (Figure 1D, E).

Interestingly, FBS/L pre-cultured C1 ESCs induced with a low amount of Doxy (TMP10μM_Doxy10ng/mL “During Differentiation” sample, Figure 1D) converted into EpiSCs more efficiently as compared to all other treatments from FBS/L (Figure 1D).

Altogether, these results indicate that both the cell culture media and levels of exogenous β-catenin strongly influence how cells respond to the ActivinA/FGF2 differentiation stimulus, with the 2i/L pre-culture enabling more homogeneous differentiation towards Epiblast, and moderate β-catenin overexpression in FBS/L-derived ESCs, during the differentiation protocol only, improving EpiSCs establishment *in vitro*.

Chemical modulation of the Canonical Wnt pathway enhances Epiblast derivation from ESCs

The above results (Figure 1) and the need to define a protocol for efficient derivation of EpiSCs *in vitro* motivated us to explore the differentiation potential of wild-type ESCs when deprived from pluripotency factors and exposed to different chemical perturbations of the Wnt/β-catenin pathway (Figure 2A). We took advantage of the *miR-290-mCherry/miR-302-eGFP*[53] ESC line (hereafter called dual reporter ESCs), which allows fluorescent tracking of the exit from pluripotency. Specifically, naïve dual reporter ESCs express the mCherry reporter only, and progressively start expressing also the GFP reporter, when allowed to differentiate into EpiSCs[53].

We measured the transition from ESCs to EpiSCs using flow cytometry in at least 2 independent 4-day time-courses (Figure 2A). Before differentiation, dual reporter ESCs were cultured in FBS/L and treated for 48 hrs with DMSO (Figure 2B) or with Chiron (1-3μM, Figure 2C, D respectively) to pre-activate the canonical Wnt pathway, or were maintained in 2i/L for 3 passages (i.e., 1 week; Figure 2E). At Day 0, 1.5×10^4 cells/cm^2 were seeded on a fibronectin-coated plate and exposed to different combination of drugs added to the NDiff227[26]: Activin+FGF2+DMSO (AFD); Activin+FGF2+Ch1μM (AFC1); Activin+FGF2+Ch3μM (AFC3); Ch1μM (C1); Ch1μM+XAV2μM (C1X2); Ch3μM (C3); Ch3μM+XAV2μM[29] (C3X2) (Figure 2A). The GFP signal was analyzed using flow cytometry every day for 4 days and the media changed after the first 2 culture days (Figure 2A).

Dual reporter ESCs pre-cultured in FBS/L in absence of β-catenin activation showed, already at Day 1, a GFP+ cell percentage increase in all but AFD treatment; AFD-treated cells efficiently transited towards the Epi state, but they were unable to rich other treatment GFP+ percentage level (Figure 2B).

FBS/L Ch1μM pre-cultured dual reporter ESCs showed an overall increased percentage of GFP+ cells compared to DMSO-treated cells (compare Figure 2B, C). However, the fold-increase at Day 4 with respect to Day 0 of the best performing conditions (i.e., C1 and C1X2; Figure 2C) was lower in Ch1μM pre-treated cells (13- and 12-fold increase, respectively; Figure 2C) in comparison with the DMSO (23- and 22-fold increase, respectively; Figure 2B). This suggests, as in the experiments performed in a β-catenin null background (Figure 1), that the ESC to EpiSC conversion is favoured by β-catenin activation during differentiation only, while its prolonged stimulation might reduce the differentiation efficiency. This was confirmed in Ch3μM

pre-treated cells, where the best performing conditions (i.e., C3 and C3X2; Figure 2D) also showed a lower percentage of GFP+ cells compared to DMSO-treated ESCs. Moreover, the simultaneous activation/inhibition of the pathway (i.e., C3X2 condition) had opposite effects given cells pre-culture conditions: the percentage of GFP+ cells increased over-time in DMSO pre-treated cells (20-fold increase at Day 4 with respect to Day 0; Figure 2B), while GFP expression was quite low at the end of the time-course in Ch3μM pre-treated cells (3.6-fold increase at Day 4 with respect to Day 0; Figure 2D). Interestingly, Chiron pre-treatment had no positive effect on the differentiation efficiency using the standard differentiation protocol (AFD), as the GFP+ percentage increase in AFD-treated cells at Day 4, as compared to Day 0, was almost the same Ch1μM pre-cultured cells (7.4-fold increase; Figure 2C) and lower in Ch3μM (1.9-fold increase; Figure 2D) and 2i/L (1.1-fold increase; Figure 2E) pre-cultured cells as compared to the DMSO condition (7.4-fold increase; Figure 2B). In cells pre-cultured in 2i/L there was not much difference across the different differentiation protocols, as can be seen by the overall higher p-values computed through a one-way ANOVA test (compare Figure 2B-E) Finally, the combined treatment with ActivinA, FGF2 and Chiron (AFC1, AFC3; Figure 2B-E) did not change EpiSCs derivation efficiency, as compared to the standard ActivinA/FGF2 treatment (Figure 2B-E).

We noticed that the efficiency of *in vitro* EpiSCs derivation strongly varied across experiments: in Supplementary Figure 2, we showed an average of at least 2 experiments where the overall percentage of GFP+ cells was almost halved across conditions, as compared to data in Figure 2. Still, we confirmed that the addition of Chiron during differentiation, in combination or not with XAV2μM (C1 and C1X2 or C3 and C3X2; Supplementary Figure 2A-D), enables a much more efficient conversion towards EpiSCs as compared to other protocols. Also, we confirmed that, if pre-cultured in FBS/L, a protocol with no pre-activation of the Wnt/β-catenin pathway and differentiation in media enriched with Ch1μM±XAV2μM enables efficient EpiSCs derivation (C1 and C1X2; Supplementary Figure 2A), in agreement with β-catenin genetic perturbation results in Figure 1.

To confirm these results at single cell level, we monitored single-cell ESC-EpiSC transition in 71 hrs time-lapse microscopy experiments (Movies 1-3; see Methods for details); FBS/L pre-cultured dual reporter ESCs were imaged every 60 minutes while constantly stimulated with AFD (Movie 1) or Chiron 1-3μM (Movies 2 and 3, respectively). In the AFD condition, a few GFP+ cells started to appear after 57 hrs

(Movie 1), whereas in the C1 and C3 culture conditions the transition started already after 10-14 hrs, with a peak around 40-43 hrs (Movies 2 and 3). The GFP signal from cells differentiated in the presence of Chiron3μM was weaker as compared to the Chiron1μM treatment (compare Movies 2 and 3).

These results confirm that strength and time of β-catenin stabilization are important to tip the balance between cell fates. In agreement with our previous observations in FBS/L pre-cultured knock-out cells (see TMP10μM_Doxy10ng/ml "During Differentiation" sample in Figure 1D), data collected using the dual reporter cell line confirm that high levels of β-catenin can be detrimental to efficiently derive EpiSCs *in vitro*. Indeed, a moderate activation or the simultaneous treatment with both an activator (i.e., Chiron) and an inhibitor (i.e., XAV) of the Wnt/β-catenin pathway improve ESC direct differentiation into EpiSCs, effectively replacing ActivinA and FGF2 requirement (Figure 2B).

Transcriptome analysis of ESC exit from pluripotency with varying β-catenin levels

Next, we studied C1 ESCs exit from 'ground state' pluripotency, i.e., upon 2i/L withdrawal, by RNA-sequencing; such monolayer differentiation protocol does not induce a specific cell fate and is ideal to observe any β-catenin dependent differentiation bias.

C1 ESCs cultured in 2i/L for 3 passages were treated for 48 hrs with saturating concentrations of Doxy and TMP (100ng/mL and 10μM, respectively) to induce the expression of the exogenous fusion protein (Figure 3A). Taking advantage of the mCherry-tag for exogenous β-catenin overexpression, Doxy/TMP treated C1 ESCs were sorted into two different subpopulations: C1 with Middle and High β-catenin levels (hereafter called C1M and C1H samples, respectively; Figure 3A and Supplementary Figure 3A). Cells were then seeded at 1.5×10^4 cells/cm^2 on gelatin-coated plates and cultured in NDiff227 media± inducers for 4 days before being transcriptionally profiled (see Methods for details; Figure 3A). Sequencing provided snapshots of the C1, C1M and C1H sample transcriptome in pluripotent condition, and of the differentiated counterparts (Day 4 samples) cultured in NDiff227 and DMSO (i.e., upon Doxy/TMP withdrawal; hereafter called C1DMV and C1DHV samples), or in NDiff227 and TMP/Doxy (hereafter called C1DMDT and C1DHDT) during

differentiation. The C1 and C1D samples refer to cells treated only with TMP10μM in the pluripotent and differentiated states, respectively.

Principal Components Analysis (PCA, Figure 3B) showed three main clusters: one group included C1, C1M and C1H in 'ground state' pluripotency, another group included C1D ESCs and the final group contained all perturbed samples (C1DMV, C1DHV, C1DMDT and C1DHDT) after 4 days of differentiation.

We next performed a Gene Ontology (GO) and Functional Annotation analysis on the differentially expressed genes, filtered for the false discovery rate (FDR<0.05) and log fold change (logFC<-2 or >2; see Methods for details). To identify gene ontologies specific for each experimental perturbation, we focused on the Biological Processes (BPs) enriched only in one comparison (red bars in Figure 3C-F, Supplementary Figure 3B, C). Starting from the pluripotent condition, when comparing C1M and C1H with C1, we found that the first 10 biological processes with a FDR<0.05 were enriched in cell cycles and metabolism (Supplementary Figure 3B, C, Supplementary Tables 1, 2). Interestingly, the genes exclusively upregulated in C1H compared to C1, belonged to tissue differentiation (i.e., eye morphogenesis and urogenital system development) and DNA methylation involved in gamete generation (Supplementary Figure 3C, Supplementary Table 2). Only a few signalling pathways involved were enriched in C1M ESCs compared to the control cell line C1 (Supplementary Tables 1, 2). These results, together with the PCA in Figure 3B, confirm previous observations about the dispensable function β-catenin has in pluripotent culture conditions[45-47,49] and suggest a bias towards differentiation in C1H ESCs (Supplementary Figure 3D, Supplementary Table 2).

We then analysed the genes differentially expressed at Day 4 upon β-catenin perturbation as compared to C1D ESCs; upregulated genes mostly contributed to the BPs significantly enriched (Figure 3C-F, Supplementary Tables 3-6), while downregulated genes only contributed to enrich general metabolic processes (e.g., regulation of transporter and cation channel activity) and mesenchymal to epithelial transition (Figure 3C-F, Supplementary Tables 3-6). Genes exclusively upregulated in the C1DMV *vs* C1D comparison belonged to the mesoderm lineage (i.e., cardiovascular system development; Figure 3C and Supplementary Table 3), while, in the C1DMDT *vs* C1D comparison, upregulated genes were enriched for the endoderm

lineage (i.e., urogenital system; Figure 3D and Supplementary Table 4). Nevertheless, mesoderm and endoderm lineages were represented in both comparisons.

GO performed on the C1DHV and C1DHDT comparisons with C1D showed only a few differences in the enriched BPs, that indeed did not define a bias toward a specific lineage (Figure 3 E, F, Supplementary Tables 5, 6). These results suggest that the major changes in the differentiation program initiated upon 2i/L withdrawal are induced by moderate β-catenin amount and are influenced by the timing of protein overexpression. The pathway enrichment analysis showed the upregulation of protein metabolism in C1DMV and C1DHV (Supplementary Tables 3, 5), MAPK signalling pathway (Supplementary Table 3) in C1DMV, and ECM-receptor interaction and PI3K-AKT signalling pathway in C1DHV (Supplementary Table 5).

To gauge insights into specific differentiation programs, we selected sets of markers for naïve and general pluripotency, early post-implantation epiblast, ectoderm, mesoderm, endoderm, germ cell and trophectoderm[51], and clustered our samples according to the expression of these gene sets.

Naïve pluripotency genes were downregulated during differentiation in all samples, indicating the successful exit of cells from pluripotency (Figure 3G). Pluripotent C1M and C1H samples clustered together (Figure 3G) although close to C1 ESCs, in agreement with previous observations (Figure 3B); ESCs differentiated in presence of DMSO (i.e., C1DMV and C1DHV; Figure 3G) clustered together, similarly to samples differentiated in presence of Doxy and TMP (i.e., C1DMDT and C1DHDT, Figure 3G). Upon 2i/L withdrawal, a large number of genes (e.g., Klf5, Tcl1, Klf2 and Nr0b1) showed a different pattern among C1D, C1DMV, and C1DHV, discriminating ESCs with different β-catenin amounts (Figure 3G) and supporting the hypothesis of a β-catenin-dependent effect on transcriptional changes.

The clustering across samples was similar for general pluripotency markers (Figure 3H). In accordance with previous reports about the transition to primed pluripotency[54-57], in the majority of differentiated samples Sox2 was downregulated and Utf1, Zfp281 and Lin28 were upregulated (Figure 3H). Moreover, almost all the genes were lower in C1DMV, C1DMDT, C1DHV and C1DHDT as compared to C1D (exceptions were Lin28a, higher in C1DHDT and Sox2, higher in C1DHV; Figure 3H), and showed different behaviours in DMSO- (i.e., C1DMV and C1DHV; Figure 3H) *vs* Doxy/TMP-treated samples (i.e., C1DMDT, C1DHDT; Figure 3H), confirming that the duration of

β-catenin overexpression has an influence on cell identity. Zfp281, Zic2 and Utf1 showed a similar pattern in β-catenin overexpressing cells as compared to C1D ESCs, all being downregulated (Figure 3H). Zfp281 is a Zinc finger transcription factor implicated in regulating stem cell pluripotency[58,59], and recently reported as a bidirectional regulator of the ESC-EpiSC transition in cooperation with Zic2, another zinc finger protein[60]. The undifferentiated embryonic cell transcription factor 1 (Utf1) is expressed in ESCs and is involved in many aspects of gene expression control (e.g., transcription factor[61] and epigenome organization[62,63]), playing an important regulatory role during the exit of ESCs from pluripotency[62,63]. The concomitant reduction of Zfp281, Zic2 and Urf1 suggests a global change in the chromatin organization of β-catenin overexpressing ESCs en route to differentiation (Figure 3H). Early post-implantation epiblast genes were mostly upregulated in primed ESCs compared to the pluripotent condition with no evident differences across treatments in naïve ESCs (Figure 3I). The exception was Foxd3, downregulated in both naïve and primed β-catenin overexpressing cells as compared to the controls C1 and C1D ESCs (Figure 3I). Interestingly, Dnmt3a levels, although similar at T0, were very different at Day 4, with C1DMV/C1DHV and C1DMDT/C1DHDT showing 80% and 70% gene expression reduction as compared to the control C1D, respectively (Figure 3I); also, samples constantly exposed to Doxy/TMP (i.e., C1DMDT and C1DHDT) showed higher Dnmt3a expression than DMSO-treated ESCs (i.e., C1DMV and C1DHV; Figure 3I). Similar observations hold for Dnmt3b, where the reduction compared to C1D was of about 60% for C1DMV/C1DHV and 10% for C1DMDT/C1DHDT; (Figure 3I). Dnmt3a, b and Foxd3 are DNA and chromatin remodelling factors, respectively; Dnmt enzymes methylate genomic regions, whereas Foxd3 reduces active and enhances inactive histone marks by recruiting the Lysine-specific demethylase 1 (Lsd1)[64]. The reduced expression of those genes, including the pluripotent markers Utf1 discussed above, supports the hypothesis of differentially methylated DNA in β-catenin overexpressing cells.

We also screened for a large panel of lineage-priming factors. Clustering based on the ectoderm lineage genes showed that pluripotent C1 and C1M are more similar than C1H (Figure 3J); following 2i/L withdrawal, the clustering resembled those of previous sets (Figure 3G-I), with C1DMV/C1DHV and C1DMDT/C1DHDT grouping together (Figure 3J). Genes from this lineage had different and sometimes opposite expression across samples, making difficult to identify a clear pattern associated with β-catenin

perturbations. Nevertheless, we distinguished two groups of genes: one group (i.e., Dlx3, Pou3f2, Otx1 and Pou3f3) was mainly downregulated during differentiation, whereas the other group (i.e., Nes, Ascl1, Cdh2 and Pax6) had the opposite trend (Figure 3J).

When looking at mesoderm markers (Figure 3K), differentiated samples clustered similarly to the previous data set, however C1DMV/C1DHV were more similar to C1D than in previous comparisons (Figure 3G-J) and genes showed different expression patterns across conditions. Lhx1, Lefty1-2, Meox1, Hoxb1 and Bmp4 were mainly upregulated upon differentiation and no major differences were observed across samples in pluripotent conditions. The exception in this group was Lhx1 that was higher in β-catenin overexpressing cells in a time-dependent manner (compare C1DMV/C1DHV with C1DMDT/C1DHDT in Figure 3K). In contrast, genes as Nodal, Kdr, Mixl1, Gsc, Foxf1 and Zic1 got downregulated when exiting pluripotency and the levels across conditions were not significantly changing (Figure 3K). Of note, although the single genes are difficult to interpret, C1D were very different from differentiated samples with overexpression of β-catenin, stressing the relevance of the latter for mesoderm specification[46].

The endoderm lineage was the one mostly influenced by β-catenin perturbations: C1D cells were unable to induce the expression of endoderm-related genes (compare C1 and C1D in Figure 3L), whereas in all perturbed ESCs their expression increased over time. As previously observed (Figure 3G-K), samples clustered together based on the duration of β-catenin overexpression rather than on its dose (i.e., C1DMV/C1DHV and C1DMDT/C1DHDT, Figure 3L). Moreover, because of the impaired differentiation C1D clustered with pluripotent samples (Figure 3L). The C1DHDT sample showed the highest expression of the 50% of the endoderm-associated genes (namely, Cxcr4, Gata4 and Sox7). Slightly different was the behaviour of Cxcr4, that decreases over time; however, its expression is indicative of definitive endoderm differentiation[65] that most probably is not happening in the short protocol we applied. These observations, together with the incapability of C1D cells to embark differentiation toward this lineage, strongly support previous knowledge about the β-catenin requirement for endoderm organization[46,66].

In the analysis of the germ cell lineage markers, all genes showed a rather heterogeneous expression pattern across samples (Figure 3M). Pluripotent C1M and C1H clustered together and close to C1, and differentiated samples clustered based

on the duration of β-catenin perturbation (i.e., C1DMV/C1DHV and C1DMDT/C1DHDT). Dazl, Prdm1 and Ddx4 showed a clearer pattern in pluripotent conditions, being upregulated in C1M and C1H compared to C1 ESCs (Figure 3M). Finally, when looking at trophectoderm markers, clustering showed similarity of C1 and C1M, as for the ectoderm and endoderm lineages (Figure 3J, L, respectively). C1DMDT and C1DHDT showed similarity for this lineage, whereas C1DMV was part of a different branch clustering with C1D; C1DHV was more closely related to C1DMDT and C1DHDT (Figure 3N). Moreover, 90% of trophectoderm genes got downregulated during differentiation (namely, Eomes, Elf3 and Cdx1); the only exception was Cdx2 that was upregulated in C1D, C1MDV and C1DMDT in comparison with the corresponding T0 (Figure 3N). Eomes was recently reported to control the exit from pluripotency by acting on the chromatin status[67]; its behaviour in naïve C1M and C1H ESCs support the theory of a different chromatin conformation in pluripotent β-catenin overexpressing cells (Figure 3N).

Accounting for the fact that ectoderm is a default linage of the monolayer differentiation protocol we applied[68], sequencing results suggest that β-catenin overexpression in a knock-out background favours rescuing defects in differentiation towards endoderm more than mesoderm. Indeed, mesodermal genes were mostly downregulated when β-catenin was overexpressed, whereas endodermal genes were all upregulated as compared to the control (Figure 3K and L). Moreover, we observed that lineage differentiation was influenced by the duration of protein overexpression rather than the dose. According to that, there was a transition from mesoderm to endoderm following moderate but constant β-catenin overexpression (compare C1DMV and C1DMDT in Figure 3C, D). Nevertheless, endoderm was an enriched gene ontology in all considered comparisons (Figure 3C-F).
Finally, the observed expression of pluripotency markers Zfp281, Zic2 and Utf1, the early post-implantation markers Dnmt3a-b and Foxd3 and the trophectoderm marker Eomes suggests a reorganization of the epigenome in naïve C1M and C1H ESCs and upon monolayer differentiation of C1DMV, C1DMDT, C1DHV and C1DHDT ESCs.

Weighted Gene Correlation Network Analysis (WGCNA) identifies the processes associated with β-catenin perturbations

Weighted Gene Correlation Network Analysis (WGCNA)[69] is a computational approach that allows the identification of gene modules based on their correlation and network-derived topological properties. We applied WGCNA to our sequencing data and identified 13 different modules (Supplementary Figure 4A; see Methods for details). We then defined the principal component of each module (i.e., eigenmodule, ME) and calculated the Pearson Correlation Coefficient (*r*) of each eigenmodule with time (Supplementary Figure 4B) or β-catenin levels (Figure 4A). Next, for each module, we performed a functional annotation analysis on the genes with a module membership |kME| ≥ 0.8 (Methods) to identify the biological processes and pathways enriched (Supplementary Table 7), focusing the attention on the modules having $r > 0.5$ and p-value < 0.05 with the examined traits (Figure 4A, Supplementary Figure 4 A, Methods).

We found four modules significantly correlating (i.e., Green r = 0.92/p-value = 9e-14, Blue r = 0.82/p-value = 1e-08 , Black r = 0.67/p-value = 3e-05 and Brown r =0.57/p-value = 7e-04; Supplementary Figure 4B, Supplementary Table 7) and three anti-correlating (i.e., Turquoise r = -0.99/p-value = 2e-24, yellow r = -0.75/p-value = 1e-06 and Pink r = -0.56/p-value = 8e-04; Supplementary Figure 4B, Supplementary Table 7) with time, meaning that these modules were regulated during the differentiation. The biological processes related to these modules with a FDR<0.05 showed an enrichment of genes involved in translation, rRNA processing, ribosomal biogenesis and stem cell division (Supplementary Figure 4C, E Supplementary Table 7, Green and Brown), protein transport and processes associated with cellular respiration (Supplementary Figure 4D, Supplementary Table 7, Blue), positive regulation of growth, ncRNA processing and neuronal tube formation and development (Supplementary Figure 4E, Supplementary Table 7, Brown), regulation of tissue remodelling, embryonic and forebrain development, stem cell population maintenance and cell homeostasis (Supplementary Figure 4F, Supplementary Table 7, Turquoise), nuclear division and meiosis and synaptonemal assembly and organization (Supplementary Figure 4G, Supplementary Table 7, Pink). For the pathway analysis, we found an enrichment in ribosome (Supplementary Table 7, Green and Blue), Hedgehog signalling pathway (Supplementary Table 7, Green), oxidative phosphorylation and diseases associated with oxidative stress (Supplementary Table 7, Blue and Turquoise), cancer (Supplementary Table 7, Brown and Turquoise) and regulation of the actin cytoskeleton (Yellow) . Of note, there were no significantly

enriched BPs and/or pathways for the genes from the Black, Yellow and Pink modules (Supplementary Table 7, Black, Yellow and Pink).

To gain more information about the effect of β-catenin overexpression levels, we correlated the eigenmodule of each module with β-catenin levels (see Methods for details) and found three modules correlating with β-catenin doses (i.e., Tan r = 0.81/p-value = 2e-8, Purple r = 0.71/p-value = 7e-6 and Yellow/Green r = 0.69/p-value =1 e-5; Figure 4A, Supplementary Table 7). The biological processes corresponding to these modules showed enrichment in cell division (Figure 4B, Supplementary Table 7, Tan), metabolism and negative regulation of neuronal death (Figure 4C, Supplementary Table 7, Purple). Finally, the pathways analysis showed a significant enrichment only in Lysosome and N-Glycan biosynthesis from the Purple module, whereas pentose phosphate pathways and autophagy from the Green/Yellow (Supplementary Table 7, Purple and GreenYellow).

The WGCNA analysis show major transcriptional and metabolic changes associated with the exit from the pluripotent status and confirmed β-catenin functions on cell survival and proliferation[31].

Discussion

The role of the Wnt/β-catenin pathway as a pluripotency gatekeeper has been matter of many debates[30,42,48,70-73]; while modulation of the canonical Wnt pathway has been extensively proved to be important for EpiSC *in vivo* derivation[74,75], self-renewal[76] and *in vitro* lineage differentiation[77-79], its relevance in the exit from pluripotency and in ESC-EpiSC direct transition have not been explored thoroughly.

In this work we proved that genetic β-catenin manipulation or chemical perturbations of the canonical Wnt pathway control ESC fate at the exit from pluripotency.

Using two different cellular models, we found that moderate β-catenin overexpression in β-catenin$^{-/-}$ ESCs or its stabilization in wild-type ESCs increase the differentiation efficiency of ESCs into EpiSCs, similarly to what was reported for EpiSCs self-renewal[29]: EpiSCs can be maintained in Chiron3μM/XAV2μM cultures, with self-renewal regulated by both Axin2 and β-catenin[29]; here we found that, in absence of pre-activation of the canonical Wnt pathway, the Chiron3μM/XAV2μM treatment has a better effect than Chiron3μM alone on ESCs-EpiSCs transition at the end of the

differentiation experiments (Day 3 and 4 in Figure 2B), while the opposite was observed in early phases of the protocol (Day 1 and 2 in Figure 2B). This could be explained by the fact that Axin2 expression is β-catenin-dependent, and β-catenin stabilization gets induced by Chiron treatment; therefore, the effect of XAV might be relevant only upon Axin2 stabilisation. Alternatively, it might also suggest a switch in the effect of Chiron3μM/XAV2μM stimulation in a specific moment during the differentiation process, probably when ESCs start to acquire a more stable EpiSC identity (as in[29]). Although both hypotheses are in agreement with what was reported by Kim and colleagues[29], the first seems to be more plausible looking at the response in Ffg5 (Figure 1) and GFP expression (Figure 2B, Supplementary Figure 2A), when a moderate activation of the Wnt/β-catenin was induced. Indeed, both β-catenin$^{-/-}$ exposed to a low concentration of the input Doxy (i.e., TMP10 μM _Doxy10ng/mL, 'During Differentiation' in Figure 1D) and the dual reporter ESCs treated with Chiron1μM (i.e., C1 in Figure 2B) showed the highest differentiation efficiency, suggesting that Chiron1μM treatment alone is enough to keep β-catenin levels within a range that would instead require XAV treatment when using higher doses of Chiron (i.e., 3μM), and that Chiron1μM is mimicking the effect obtained by β-catenin genetic manipulation. Furthermore, XAV treatment in combination with Chiron1μM reduced the % of differentiated cells at Day 1; this could be due to the stoichiometry between β-catenin, Ainx2 and the two inhibitors. We reason that, in Chiron1μM/XAV2μM, XAV is in excess with respect to the amount of transcribed Axin2, therefore all the translated protein gest stabilised, and the final effect is a strong inhibition of the signalling pathway. Nevertheless, this effect might get attenuated with time, probably when a balance between the drug and the target is achieved. This theory seems to be supported by the behaviour of cells treated with Chiron1μM or Chiron3μM; the first showed a GFP peak within the first 2 days followed by GFP stabilisation, while the second showed the opposite trend (i.e., a reduction over time), suggesting prolonged β-catenin stabilization in FBS/L can impair ESCs differentiation. This poses the question of what would have happened if cells were stimulated for longer with Chiron1μM. There are two possible scenarios; in the first, EpiSCs, derived from ESCs, would self-renew in Chiron1μM as well as in Chiron3μM/XAV2μM. In the second scenario, the transition from Chiron1μM to Chiron 3μM would be preferred for the maintenance of established EpiSCs. However, the latter would be in contrast with the results showed in[29], where they proved immediate differentiation or death of EpiSCs

expanded in Chiron3μM±PD1μM. Of note, the basal medium used in[29] for EpiSCs self-renewal is based on GMEM supplemented with 10% FBS[29], therefore differences might be expected. Finally, we found that 2i/L pre-cultured ESCs better differentiate into EpiSCs, regardless of further modulation of the pathway during the differentiation process.

Overall, these results confirm the effect β-catenin has on differentiation and suggest that both the duration and the dose of β-catenin overexpression have an effect on cell differentiation *in vitro*. Moreover, we defined an improved protocol for EpiSCs derivation *in vitro*, based on NDiff227 and Chiron1μM.

These observations are supported by the RNA sequencing performed in ESCs during the exit from the naïve ground state pluripotency[51]. In β-catenin overexpressing cells (in particular in C1DMV), Dnmt3a and b showed a pattern similar to the one observed in Rex1-high ESCs differentiated using a similar protocol[51], clearly indicating that moderate β-catenin overexpression in naïve ESCs influences DNA methylation associated with the exit from pluripotency. Interestingly, we observed a significant upregulation of endodermal genes in β-catenin overexpressing cells, indicating a requirement of β-catenin for this specific fate. This phenotype was previously reported in the β-catenin null cell line generated by Lyashenko and colleagues[46], where the defect in the endoderm lineage was also rescued by overexpressing both wild-type or transcriptional incompetent β-catenin[46].In contrast, mesoderm and ectoderm induction seem to not require β-catenin[46]. With our approach that enables dose- and time-controlled β-catenin overexpression, we were able to define the amount of protein and the optimal window of overexpression to facilitate mesoderm (i.e., C1DMV; Figure 3D, Supplementary Table 3) or endoderm (i.e., C1DMDT; Figure 3E, Supplementary Table 4) differentiation, and confirmed that the ectoderm lineage is not affected by β-catenin loss and therefore is not influenced by its overexpression.

In the future, it will be of great interest to use this inducible system to interrogate the effect of more complex β-catenin dynamics on stem-cell identity and to further investigate the role of the β-catenin transcriptional activity in pluripotent and differentiated cells of both murine and human origin.

Authors Contributions

E.P. designed and performed experiments; M.F. and G.G. performed the WGNCA analysis; M.F. performed the GO; R.D.C. performed the Differential Expression analysis; E.P., and L.M. analysed data; E.P., M.F., R.D.C. and L.M. wrote the paper; D.d.B. supervised the bioinformatics analysis; L.M. supervised the entire project.

Acknowledgements

We thank Dr Robert Blelloch for the *miR-290-mCherry/miR-302-eGFP* ESC line; Dr Andre Hermann and Dr Lorena Sueiro Ballesteros (Flow Cytometry Facility, University of Bristol), Dr Mark Jepson and Alan Leard (Wolfson Imaging Facility, University of Bristol) and the Next Generation Sequencing Core (TIGEM, Naples) for their support. This work was funded by Medical Research Council (grant MR/N021444/1) to L.M., by the Engineering and Physical Sciences Research Council (grants EP/R041695/1 and EP/S01876X/1 to L.M.), EC funding H2020 (FET OPEN 766840-COSY-BIO) to L.M., BrisSynBio, a BBSRC/EPSRC Synthetic Biology Research Centre (BB/L01386X/1) to L.M, STAR-University of Naples Federico II grant to GG and Fondazione Telethon grant to DdB.

Methods

Cell line derivation

C1 cell lines were previously derived in[49] by a double lentiviral infection of β-catenin$^{-/-}$ ESCs[45] with the EF1a-rtTA (Neomycin) plasmid followed by the pLVX_TrE3G-DDmCherryβ-catenin^{S33Y}(Puromycin). Cells were selected with Neomycin after the first round and with Puromycin after the last infection. The dual reporter ESCs were a gift from Dr Blelloch[53].

ESCs were cultured on gelatine-coated dishes in Dulbecco's modified Eagle's medium (DMEM) supplemented with 15% fetal bovine serum (FBS, Sigma), 1 x nonessential amino acids, 1 x GlutaMax, 1 x2-mercaptoethanol and 1000 U/mL LIF (Peprotech). To note, that for the 2i/L culture, cells were kept for 3 passages (around 1week) in serum-free NDiff227-based media supplemented with 1000 U/mL LIF, 3μM of the GSK-3α/β inhibitor Chiron-99021 (Selleck, S1263) and 1μM of the MEK inhibitor PD0325901 (Selleck, S1036).

Epiblast Differentiation

For EpiSC derivation *in vitro*, FBS/L and 2i/L 1.5×10^4 cells/cm^2 were seeded on 10µg/mL Fibronectin-coated 12-well plates in NDiff227 (Takara, Y40002) and, according to the experiment, stimulated with DMSO, TMP10µM (Sigma, T7883), Doxy 10-100ng/mL (Sigma, D9891), human ActivinA 10ng/mL (Peptrotech, 120-14E), human FGF2 10ng/mL (Peptrotech, 100-18B) Chiron1-3µM and the XAV939 2µM (Sigma, 575545) for 4 days with the media and drugs refreshed after the first 2 days (Figures 1B, C and 2A).

Monolayer differentiation

Sorted C1, C1M and C1H ESCs were plated at 1.5×10^4 cells/cm^2 on gelatine-coated 12-well plates in plain NDiff227 and stimulated with DMSO or TMP10µM±Doxy 10-100ng/mL for 4 days with the media and drugs refreshed after the first 2 days (Figure 3A).

Drugs pre-treatment

Some experimental conditions required pre-treatment of cells. For β-catenin overexpression in Figure 1C, C1 ESCs were stimulated for 48 hrs with TMP10µM and Doxy 10-100ng/mL before the EpiSC differentiation, whereas for pre-activation of the canonical Wnt pathway in Figure 2A, C-E and Supplementary Figure 2B-D, dual reported ESCs were exposed to Chiron1-3µM (Figure 2C, Supplementary Figure 2B and Figure 2D, Supplementary Figure 2C, respectively) for 48 hrs or cultured for 3 passages in 2i/L (Figure 2E, Supplementary Figure 2D), before the differentiation.

Flow cytometry analysis

ESCs from a 12-well plate were washed with sterile Phosphate-Buffered Saline (PBS, Gibco), incubated with 80 µL of trypsin for 2–3′ at room temperature and collected with 120 µL of PBS 2% FBS containing DAPI as cell viability marker. Cell suspension was analysed using the BD LSR Fortessa and 10,000 living cells were recorded for each sample. The % of GFP positive cells was calculated over living cells, gated as DAPI negative, using the FlowJo V10 software.

Flow activated cell sorting (FACS)

ESCs were washed with sterile phosphate-buffered saline (PBS, Gibco), trypsinised for 2–3′ at room temperature and centrifuged at 1000 × g for 5′. Pelleted cells were

resuspended in 500 µL of plain NDiff227 media supplemented with DAPI. The mCherry positive fraction was sorted from DAPI negative using the BD Influx high-speed 16-parameter fluorescence activated cell sorter.

qPCR

For quantitative PCR, the total RNA, extracted from cells using the RNeasy kit (Qiagen), was retrotranscribed (Thermo Fischer, RevertAid Reverse Transcriptase EP0441) and the cDNA used as template for each qPCR reaction in a 15 µL reaction volume. iTaq Universal SYBR Green Supermix (1725120, Bio-Rad) was used with the Qiagen Rotor-Gene System. To eliminate the contamination from genomic DNA, the RNeasy Plus Mini Kit (Qiagen, 74134) was used to purify the total RNA used for the RNA Sequencing. The primers used were: Actin-Fwd: ACGTTGACATCCGTAAAGACCT, Actin-Rev: GCAGTAATCTCCTTCTGCATCC; Fgf5-Fwd: AAAACCTGGTGCACCCTAGA, Fgf5-Rev: CATCACATTCCCGAATTAAGC).

Time-Lapse

1.5×10^4 cells were seeded on 10µg/mL fibronectin-coated µ-Slide 8 Well Glass Bottom (Ibidi, 80827) and imaged with a Leica DMI6000 inverted epifluorescence microscope equipped with the Photometrics Prime 95B sCMOS camera (1200x1200 11µm pixels, 8 ,12 bit or 16 bit, 70 fps full frame) and an environmental control chamber (Solent) for long- term temperature control and CO2 enrichment. The Adaptive Focus Control (AFC) ensures focus is maintained during multiple acquisition cycles. Images were acquired from two channels (phase contrast and green fluorescence) with a 20X objective every 60min for 71 hrs. ImageJ version: 2.0.0-rc-69/1.52p was used to improve the GFP signal, apply a Gaussian blur filter (Sigma radius 2) and combine channels.

QuantSeq 3’ RNA sequencing library preparation.

Preparation of libraries was performed with a total of 100ng of RNA from each sample using QuantSeq 3'mRNA-Seq Library prep kit (Lexogen, Vienna, Austria) according to manufacturer's instructions. Total RNA was quantified using the Qubit 2.0 fluorimetric Assay (Thermo Fisher Scientific). Libraries were prepared from 100ng of total RNA using the QuantSeq 3' mRNA-Seq Library Prep Kit FWD for Illumina

(Lexogen GmbH). Quality of libraries was assessed by using screen tape High sensitivity DNA D1000 (Agilent Technologies). Libraries were sequenced on a NovaSeq 6000 sequencing system using an S1, 100 cycles flow cell (Illumina Inc.). Amplified fragmented cDNA of 300 bp in size were sequenced in single-end mode with a read length of 100 bp.

Illumina novaSeq base call (BCL) files are converted in fastq file through bcl2fastq [http://emea.support.illumina.com/content/dam/illuminasupport/documents/documentation/software_documentation/bcl2fastq/bcl2fastq2-v2-20-software-guide-15051736-03.pdf] (version v2.20.0.422).

QuantSeq 3' RNA sequencing data processing and analysis.

For analysis, sequence reads were trimmed using bbduk software (https://jgi.doe.gov/data-and-tools/bbtools/bb-tools-user-guide/usage-guide/) (bbmap suite 37.31) to remove adapter sequences, poly-A tails and low-quality end bases (regions with average quality below 6). Alignment was performed with STAR 2.6.0a3[80] on mm10 reference assembly obtained from cellRanger website (https://support.10xgenomics.com/single-cell-gene-expression/software/release-notes/build#mm10_3.0.0; Ensembl assembly release 93). Expression levels of genes were determined with htseq-count[81] using Gencode/Ensembl gene model. We have filtered out all genes having<1 cpm in less than n_min samples and Perc MM reads>20% simultaneously. Differential expression analysis was performed using edgeR[82], a statistical package based on generalized linear models, suitable for multifactorial experiments. The threshold for statistical significance chosen was False Discovery Rate (FDR)<0.05 (GSE148879). The lists of differentially expressed genes (DEGs), for each comparison, with a threshold of logFC>2 for the induced and logFC<-2 for the inhibited transcripts (Supplementary Tables 1-6) were used for the Functional Annotation analysi.

The data were deposited in GEO with the accession number GSE148879.

Weighted Gene Correlation Network Analysis (WGCNA)

Quant-seq 3' mRNA data of 32 samples was used to construct a gene co-expression network by applying Weighted Gene Correlation Network Analysis (WGCNA)[69] from the WGCNA package in the R statistical environment version 3.6. Briefly, we first computed the Pearson correlation coefficient among all pairs of expressed genes and

then an appropriate value of the soft-thresholding power (β=6) giving a scale-free topology fitting index (R^2) ≥ 0.85 was selected to build the weighted adjacency matrix. The weighted adjacency matrix was further transformed into a topological overlap matrix (TOM)[83] and the resulting dissimilarity matrix used for hierarchical clustering. Gene modules were finally identified by cutting the hierarchical dendrogram with the dynamic tree cut algorithm from dynamicTreeCut package in R[84] statistical environment with standard parameters, except for cutHeight we set equal to 0.25 and deepSplit we set equal to 1. The value of deepSplit parameter was selected after performing a cluster stability analysis. Briefly, for each possible value of deepSplit parameter (i.e., 0, 1, 2, 3 or 4), modules were identified for both the full dataset and 50 resampled datasets. Then, the clustering solution obtained for the full dataset was compared with each resampled solution by mean of Adjusted Rand Index (ARI)[85]. The solution giving the highest average ARI was used for the clustering analysis as described above. Finally, to identify which clusters were correlated with β-catenin expression levels or differentiation time we correlated the first principal component of each gene module (i.e., the eigenmodule) with the traits of interest. The eigenmodule can be considered as a "signature" of the module gene expression. Modules correlated with the traits with a p-value<0.01 were considered statistically significant and used for further analyses.

Functional Annotation Analysis

Differentially expressed genes (either logFC>2 or logFC<-2) and module "hubs" having high module membership (also known as |KME|>0.8) within the module were analysed for the enrichment in GO Biological Processes[86] and KEGG Pathways[87] via the clusterProfiler package in R statistical environment[88]. The threshold for statistical significance was FDR<0.05, the top-ten BPs were represented as -log10 (FDR; Figures 3C-F, Supplementary Figure 3B, C and Figure 4B, C, Supplementary Figure 4C-G.

Statistical analysis

Differences between samples were analysed by two-tailed unpaired t and one-way ANOVA using Matlab (MathworksMatlab R2019a, update 9.6.0.1307630). A p-value lower than 0.05 was considered statistically significant.

Clustergram over heatmaps were generated using the clustergram function in Matlab (MathworksMatlab R2019a, update 9.6.0.1307630) that applies the Euclidean distance metric and average linkage. The data have been standardized across all samples for each gene and have 0 as mean and 1 as standard deviation.

Figure Legends

Figure 1. Dual-input control of β-catenin levels in EpiSC derivation *in vitro*.

A Dual-input regulation system consisting of the doxycycline responsive element and the conditionally destabilised mCherryβ-catenin^{S33Y} module. Doxycycline (Doxy) and trimethoprim (TMP) allow mCherryβ-catenin^{S33Y} transcription initiation and protein stabilisation, respectively. **(A, inset)** Flow cytometry profile of C1 ESCs treated for 24 hrs with TMP10μM and the indicated concentrations of Doxy. **B, C** Experimental scheme ESC to EpiSC differentiation. FBS/L and 2i/L C1 ESCs were pre-treated either with DMSO **(B)** or TMP10μM and Doxy10-100ng/mL **(C)**. Following 48 hrs of treatment, cells were seeded on fibronectin in NDiff227 and exposed to ActvinA/FGF2 and different combination of DMSO, Doxy and TMP for 4 days before being collected for RNA extraction. After 2 days, the media was changed, and the drugs were refreshed. **D, E** Fgf5 mRNA levels measured in FBS/L **(D)** and 2i/L **(E)** C1 ESCs, after 4 days of differentiation in NDiff227+ActivinA/FGF2 and different combination of DMSO, Doxy and TMP. Data are means ± SEM (n=7, D (T0, Doxy10-100ng/mL "During Differentiation", Doxy10ng/mL T0, Doxy100ng/mL T0, Doxy100ng/mL "Before" ad Doxy100ng/mL "Always"); n=6, D (Doxy10ng/mL "Before"); n=5, D (TMP10μM "During Differentiation"); n=2, E). p-values from two-tailed unpaired t test computed by comparing each sample with C1 TMP10μM "During Differentiation" are shown, *p<0.05, **p<0.01, ***p<0.001, ****p<0.0001. Dots represent individual data with similar values overlapping.

Figure 2. Chemical perturbation of the Wnt/β-catenin in EpiSC **derivation *in vitro*.**

A Experimental scheme of Epiblast differentiation. Dual reporter ESCs cultured in FBS/L and pre-treated for 48 hrs with DMSO and Chiron (1-3 μM), or in 2i/L for 3 passages, were seeded on fibronectin in NDiff227 supplemented with different combination of drugs (Activin+FGF2+DMSO (AFD); Activin+FGF2+Ch1μM (AFC1); Activin+FGF2+Ch3μM (AFC3); Ch1μM (C1); Ch1μM+XAV2μM (C1X2); Ch3μM (C3); Ch3μM+XAV2μM (C3X2)). The GFP signal from the EpiSC marker was measured by

flow cytometry every 24 hrs for 4 consecutive days. After the first 2 days, the media was changed, and the drugs were refreshed. **B-E** Percentage of GFP+ cells calculated over the total amount of living cells in DMSO **(B)**, Ch1μM **(C)**, Ch3μM **(D)** and 2i/L **(E)** pre-cultured dual reporter ESCs. Histograms from Day 0 and Day 4 of each condition are shown as insets. Data are means ± SEM (n=2, B (Day1, Day3 AFD, Day4 AFD), C (Day 1), D (Day1, Day3 AFC3), E (Day0, Day1 AFC3-C3X2); n=3, B (Day0, Day2, Day3 AFC1-AFC3-C1-C1X2-C3-C3X2, Day4 AFC1-AFC3-C1-C1X2-C3-C3X2), C (Day0, Day2 AFD-AFC1-C1X2, Day3, Day4), D (Day0, Day2 AFD-AFC3-C3X2, Day3 AFD-C3-C3X2, Day4), E (Day1 AFD, Day2 AFD-AFC3-C3X2, Day3, Day4); n=6, C (Day2 C1), D (Day2 C3), E (Day1 C3, Day2 C3). p-values from one-way ANOVA are shown across samples for each day. Dots represent individual data with similar values overlapping. Colour-blind safe combinations were selected using colorbrewer2 (https://colorbrewer2.org/#type=sequential&scheme=BuGn&n=3).

Supplementary Figure 2. Replica of *in vitro* ESC-EpiSC differentiation experiments upon chemical β-catenin perturbations

A-D Percentage of GFP+ cells calculated over the total amount of leaving cells in DMSO **(B)**, Ch1μM **(C)**, Ch3μM **(D)** and 2i/L **(E)** pre-cultured dual reporter ESCs. Histograms from Day 0 and Day 4 of each condition are shown as inset. Data are means ± SEM (n=2, A (Day1 C1, Day3 AFC1, Day4 AFD-AFC3), B (Day 1 AFC1), D (Day4 AFD); n=3, A (Day1 AFD-AFC1-AFC3-C1X2-C3-C3X2, Day2, Day3 AFD-AFC3-C1-C1X2-C3-C3X2, Day4 AFC1-C1-C1X2-C3-C3X2), B (Day1 AFD-C1-C1X2, Day2, Day3, Day4), C (Day1, Day2, Day3, Day4), D (Day0, Day1, Day2, Day3, Day4); n=6, A (Day0), B (Day0), C (Day0). p-values from one-way ANOVA are shown across samples for each day. Dots represent individual data with similar values overlapping. Colour-blind safe combinations were selected using colorbrewer2 (https://colorbrewer2.org/#type=sequential&scheme=BuGn&n=3).

Figure 3. Transcriptome analysis of monolayer differentiation experiments upon β-catenin perturbations

A Experimental scheme of monolayer differentiation protocol. 2i/L C1 ESCs were pre-treated with TMP10μM and Doxy100ng/mL for 48 hrs; living cells were then sorted from the Dapi negative fraction of TMP-treated cells (C1), whereas β-catenin

overexpressing cells from Doxy/TMP-treated samples were FACS-sorted from the mCherry fraction and divided into Middle (C1M) and High (C1H) subpopulations. 1.5×10^4 cells/cm^2 from each individual population were then seeded on gelatine in NDiff227 medium supplemented with DMSO or TMP±Doxy100ng/mL. After 4 days of differentiation in NDiff227, cells were collected and processed for the RNA sequencing. During the protocol, the media was changed, and the drugs refreshed after 2 days. **B** Principal Component Analysis (PCA) of all samples; the average of biological replica is shown. **C-F** Bar-chart of the top-ten enriched biological processes (BP) with a FDR<0.05 from differentially expressed genes in C1DMV **(C),** C1DMDT **(D),** C1DHV **(E)** and C1DHDT **(F)** compared to C1D ESCs. Black and grey bars represent upregulated and downregulated BPs, respectively. In red bars, the BPs exclusively enriched in the indicated condition. **G-N** Clustergram over heatmaps of Naïve **(G)** and general pluripotency **(H)**, early post-implantation **(I)**, ectoderm **(J)**, mesoderm **(K)**, endoderm **(L)**, germ cell **(M)** and trophectoderm **(N)** lineages from pluripotent and differentiated ESCs expressing different β-catenin amount. Each column is the average of 4 biological replicates.

Supplementary Figure 3. FACS gating strategy and Gene Ontology.

A Gating strategy used to sort C1M and C1H ESCs, following 48 hrs treatment with TMP10μM and Doxy100ng/mL. C1 ESCs treated with TMP10μM were used as negative control. **B, C** Bar-chart of the top-ten enriched biological processes (BP) with a FDR<0.05 from differentially expressed genes in in C1M **(B)** and C1H **(C)** compared to C1 ESCs. Black and grey bars represent upregulated and downregulated BPs, respectively. In red bars, the BPs exclusively enriched in the indicated condition.

Figure 4. WGCNA of the genes correlating with β-catenin levels.

A Eigenmodules correlating with β-catenin amount; the Pearson Correlation Coefficient (*r)* and relative p-value are shown. **B, C** Bar-chart of the top-ten enriched biological processes (BP) with a FDR<0.05 from genes belonging to the Tan **(B)** and Purple **(C)** WGCNA modules.

Supplementary Figure 4. WGCNA of the genes correlating with time.

A Clustering dendrogram of genes, with dissimilarity based on topological overlap, together with the assigned module colours**;** grey genes are unassigned to any module**.**

B Eigenmodules correlating with time; the Pearson correlation coefficient (*r*) and relative p-value are shown. **C-G** Bar-chart of the top-ten enriched biological processes (BP) with a FDR<0.05 from genes belonging to the Green (**C)**, Blue **(D**), Brown **(E)**, turquoise **(F)** and Pink **(G)** WGCNA modules.

Supplementary Table 1

Total list of differentially expressed genes before and after the filtering for the FDR (<0.05) and log fold change (-2>log>2); GO and pathway analysis in pluripotent C1M vs C1 ESCs.

Supplementary Table 2

Total list of differentially expressed genes before and after the filtering for the FDR (<0.05) and log fold change (-2>log>2); GO and pathway analysis in pluripotent C1H vs C1 ESCs.

Supplementary Table 3

Total list of differentially expressed genes before and after the filtering for the FDR (<0.05) and log fold change (-2>log>2); GO and pathway analysis in differentiated C1DMV vs C1D ESCs.

Supplementary Table 4

Total list of differentially expressed genes before and after the filtering for the FDR (<0.05) and log fold change (-2>log>2); GO and pathway analysis in differentiated C1DMDT vs C1D ESCs.

Supplementary Table 5

Total list of differentially expressed genes before and after the filtering for the FDR (<0.05) and log fold change (-2>log>2); GO and pathway analysis in differentiated C1HV vs C1D ESCs.

Supplementary Table 6

Total list of differentially expressed genes before and after the filtering for the FDR (<0.05) and log fold change (-2>log>2); GO and pathway analysis in differentiated C1DHDT vs C1D ESCs.

Supplementary Table 7

Total list of identified module genes correlating with time (Supplementary Figure 4) or β-catenin levels (Figure 4) before and after the filtering for the |kME| ≥ 0.8; GO and pathway analysis.

References

1 Evans, M. J. & Kaufman, M. H. Establishment in culture of pluripotential cells from mouse embryos. *Nature* **292**, 154-156, doi:10.1038/292154a0 (1981).

2 Martin, G. R. Isolation of a pluripotent cell line from early mouse embryos cultured in medium conditioned by teratocarcinoma stem cells. *Proc Natl Acad Sci U S A* **78**, 7634-7638, doi:10.1073/pnas.78.12.7634 (1981).

3 Ying, Q. L. *et al.* The ground state of embryonic stem cell self-renewal. *Nature* **453**, 519-523, doi:10.1038/nature06968 (2008).

4 Brook, F. A. & Gardner, R. L. The origin and efficient derivation of embryonic stem cells in the mouse. *Proc Natl Acad Sci U S A* **94**, 5709-5712, doi:10.1073/pnas.94.11.5709 (1997).

5 Williams, R. L. *et al.* Myeloid leukaemia inhibitory factor maintains the developmental potential of embryonic stem cells. *Nature* **336**, 684-687, doi:10.1038/336684a0 (1988).

6 Smith, A. G. *et al.* Inhibition of pluripotential embryonic stem cell differentiation by purified polypeptides. *Nature* **336**, 688-690, doi:10.1038/336688a0 (1988).

7 Ying, Q. L., Nichols, J., Chambers, I. & Smith, A. BMP induction of Id proteins suppresses differentiation and sustains embryonic stem cell self-renewal in collaboration with STAT3. *Cell* **115**, 281-292, doi:10.1016/s0092-8674(03)00847-x (2003).

8 Niwa, H., Burdon, T., Chambers, I. & Smith, A. Self-renewal of pluripotent embryonic stem cells is mediated via activation of STAT3. *Genes Dev* **12**, 2048-2060, doi:10.1101/gad.12.13.2048 (1998).

9 Matsuda, T. *et al.* STAT3 activation is sufficient to maintain an undifferentiated state of mouse embryonic stem cells. *EMBO J* **18**, 4261-4269, doi:10.1093/emboj/18.15.4261 (1999).

10 Marucci, L. *et al.* beta-catenin fluctuates in mouse ESCs and is essential for Nanog-mediated reprogramming of somatic cells to pluripotency. *Cell Rep* **8**, 1686-1696, doi:10.1016/j.celrep.2014.08.011 (2014).

11 Boroviak, T. *et al.* Lineage-Specific Profiling Delineates the Emergence and Progression of Naive Pluripotency in Mammalian Embryogenesis. *Dev Cell* **35**, 366-382, doi:10.1016/j.devcel.2015.10.011 (2015).

12 Marks, H. *et al.* The transcriptional and epigenomic foundations of ground state pluripotency. *Cell* **149**, 590-604, doi:10.1016/j.cell.2012.03.026 (2012).

13 Godwin, S. *et al.* An extended model for culture-dependent heterogenous gene expression and proliferation dynamics in mouse embryonic stem cells. *NPJ Syst Biol Appl* **3**, 19, doi:10.1038/s41540-017-0020-5 (2017).

14 Ghimire, S. *et al.* Comparative analysis of naive, primed and ground state pluripotency in mouse embryonic stem cells originating from the same genetic background. *Sci Rep* **8**, 5884, doi:10.1038/s41598-018-24051-5 (2018).

15 Ficz, G. *et al.* FGF signaling inhibition in ESCs drives rapid genome-wide demethylation to the epigenetic ground state of pluripotency. *Cell Stem Cell* **13**, 351-359, doi:10.1016/j.stem.2013.06.004 (2013).

16 Habibi, E. *et al.* Whole-genome bisulfite sequencing of two distinct interconvertible DNA methylomes of mouse embryonic stem cells. *Cell Stem Cell* **13**, 360-369, doi:10.1016/j.stem.2013.06.002 (2013).

17 Leitch, H. G. *et al.* Naive pluripotency is associated with global DNA hypomethylation. *Nat Struct Mol Biol* **20**, 311-316, doi:10.1038/nsmb.2510 (2013).

18 Nichols, J. & Smith, A. Pluripotency in the embryo and in culture. *Cold Spring Harb Perspect Biol* **4**, a008128, doi:10.1101/cshperspect.a008128 (2012).

19 Alexandrova, S. *et al.* Selection and dynamics of embryonic stem cell integration into early mouse embryos. *Development* **143**, 24-34, doi:10.1242/dev.124602 (2016).

20 Tesar, P. J. *et al.* New cell lines from mouse epiblast share defining features with human embryonic stem cells. *Nature* **448**, 196-199, doi:10.1038/nature05972 (2007).

21 Brons, I. G. *et al.* Derivation of pluripotent epiblast stem cells from mammalian embryos. *Nature* **448**, 191-195, doi:10.1038/nature05950 (2007).

22 Han, D. W. *et al.* Epiblast stem cell subpopulations represent mouse embryos of distinct pregastrulation stages. *Cell* **143**, 617-627, doi:10.1016/j.cell.2010.10.015 (2010).

23 Stavridis, M. P., Lunn, J. S., Collins, B. J. & Storey, K. G. A discrete period of FGF-induced Erk1/2 signalling is required for vertebrate neural specification. *Development* **134**, 2889-2894, doi:10.1242/dev.02858 (2007).

24 Kunath, T. *et al.* FGF stimulation of the Erk1/2 signalling cascade triggers transition of pluripotent embryonic stem cells from self-renewal to lineage commitment. *Development* **134**, 2895-2902, doi:10.1242/dev.02880 (2007).

25 Greber, B. *et al.* Conserved and divergent roles of FGF signaling in mouse epiblast stem cells and human embryonic stem cells. *Cell Stem Cell* **6**, 215-226, doi:10.1016/j.stem.2010.01.003 (2010).

26 Guo, G. *et al.* Klf4 reverts developmentally programmed restriction of ground state pluripotency. *Development* **136**, 1063-1069, doi:10.1242/dev.030957 (2009).

27 Johansson, B. M. & Wiles, M. V. Evidence for involvement of activin A and bone morphogenetic protein 4 in mammalian mesoderm and hematopoietic development. *Mol Cell Biol* **15**, 141-151, doi:10.1128/mcb.15.1.141 (1995).

28 Yao, S. *et al.* Long-term self-renewal and directed differentiation of human embryonic stem cells in chemically defined conditions. *Proc Natl Acad Sci U S A* **103**, 6907-6912, doi:10.1073/pnas.0602280103 (2006).

29 Kim, H. *et al.* Modulation of beta-catenin function maintains mouse epiblast stem cell and human embryonic stem cell self-renewal. *Nat Commun* **4**, 2403, doi:10.1038/ncomms3403 (2013).

30 Sato, N., Meijer, L., Skaltsounis, L., Greengard, P. & Brivanlou, A. H. Maintenance of pluripotency in human and mouse embryonic stem cells through activation of Wnt signaling by a pharmacological GSK-3-specific inhibitor. *Nat Med* **10**, 55-63, doi:10.1038/nm979 (2004).

31 De Jaime-Soguero, A. *et al.* Wnt/Tcf1 pathway restricts embryonic stem cell cycle through activation of the Ink4/Arf locus. *PLoS Genet* **13**, e1006682, doi:10.1371/journal.pgen.1006682 (2017).

32 Stamos, J. L. & Weis, W. I. The beta-catenin destruction complex. *Cold Spring Harb Perspect Biol* **5**, a007898, doi:10.1101/cshperspect.a007898 (2013).

33 Jho, E. H. *et al.* Wnt/beta-catenin/Tcf signaling induces the transcription of Axin2, a negative regulator of the signaling pathway. *Mol Cell Biol* **22**, 1172-1183, doi:10.1128/mcb.22.4.1172-1183.2002 (2002).

34 Chia, I. V. & Costantini, F. Mouse axin and axin2/conductin proteins are functionally equivalent in vivo. *Mol Cell Biol* **25**, 4371-4376, doi:10.1128/MCB.25.11.4371-4376.2005 (2005).

35 Leung, J. Y. *et al.* Activation of AXIN2 expression by beta-catenin-T cell factor. A feedback repressor pathway regulating Wnt signaling. *J Biol Chem* **277**, 21657-21665, doi:10.1074/jbc.M200139200 (2002).

36 Glinka, A. *et al.* Dickkopf-1 is a member of a new family of secreted proteins and functions in head induction. *Nature* **391**, 357-362, doi:10.1038/34848 (1998).

37 Pedone, E. & Marucci, L. Role of beta-Catenin Activation Levels and Fluctuations in Controlling Cell Fate. *Genes (Basel)* **10**, doi:10.3390/genes10020176 (2019).

38 Aulicino, F., Theka, I., Ombrato, L., Lluis, F. & Cosma, M. P. Temporal perturbation of the Wnt signaling pathway in the control of cell reprogramming is modulated by TCF1. *Stem Cell Reports* **2**, 707-720, doi:10.1016/j.stemcr.2014.04.001 (2014).

39 Ho, R., Papp, B., Hoffman, J. A., Merrill, B. J. & Plath, K. Stage-specific regulation of reprogramming to induced pluripotent stem cells by Wnt signaling and T cell factor proteins. *Cell Rep* **3**, 2113-2126, doi:10.1016/j.celrep.2013.05.015 (2013).

40 Kimura, M., Nakajima-Koyama, M., Lee, J. & Nishida, E. Transient Expression of WNT2 Promotes Somatic Cell Reprogramming by Inducing beta-Catenin Nuclear Accumulation. *Stem Cell Reports* **6**, 834-843, doi:10.1016/j.stemcr.2016.04.012 (2016).

41 Lluis, F., Pedone, E., Pepe, S. & Cosma, M. P. Periodic activation of Wnt/beta-catenin signaling enhances somatic cell reprogramming mediated by cell fusion. *Cell Stem Cell* **3**, 493-507, doi:10.1016/j.stem.2008.08.017 (2008).

42 Anton, R., Kestler, H. A. & Kuhl, M. Beta-catenin signaling contributes to stemness and regulates early differentiation in murine embryonic stem cells. *FEBS Lett* **581**, 5247-5254, doi:10.1016/j.febslet.2007.10.012 (2007).

43 Soncin, F. *et al.* Abrogation of E-cadherin-mediated cell-cell contact in mouse embryonic stem cells results in reversible LIF-independent self-renewal. *Stem Cells* **27**, 2069-2080, doi:10.1002/stem.134 (2009).

44 Wagner, R. T., Xu, X., Yi, F., Merrill, B. J. & Cooney, A. J. Canonical Wnt/beta-catenin regulation of liver receptor homolog-1 mediates pluripotency gene expression. *Stem Cells* **28**, 1794-1804, doi:10.1002/stem.502 (2010).

45 Aulicino, F. *et al.* Canonical Wnt pathway controls mESCs self-renewal through inhibition of spontaneous differentiation via β-catenin/TCF/LEF functions. *bioRxiv*, doi:10.1101/661777 (2019).

46 Lyashenko, N. *et al.* Differential requirement for the dual functions of beta-catenin in embryonic stem cell self-renewal and germ layer formation. *Nat Cell Biol* **13**, 753-761, doi:10.1038/ncb2260 (2011).

47 Wray, J. *et al.* Inhibition of glycogen synthase kinase-3 alleviates Tcf3 repression of the pluripotency network and increases embryonic stem cell resistance to differentiation. *Nat Cell Biol* **13**, 838-845, doi:10.1038/ncb2267 (2011).

48 Kielman, M. F. *et al.* Apc modulates embryonic stem-cell differentiation by controlling the dosage of beta-catenin signaling. *Nat Genet* **32**, 594-605, doi:10.1038/ng1045 (2002).

49 Pedone, E. *et al.* A tunable dual-input system for on-demand dynamic gene expression regulation. *Nat Commun* **10**, 4481, doi:10.1038/s41467-019-12329-9 (2019).

50 Sadot, E. *et al.* Regulation of S33/S37 phosphorylated beta-catenin in normal and transformed cells. *J Cell Sci* **115**, 2771-2780 (2002).

51 Kalkan, T. *et al.* Tracking the embryonic stem cell transition from ground state pluripotency. *Development* **144**, 1221-1234, doi:10.1242/dev.142711 (2017).

52 Choi, J. *et al.* Prolonged Mek1/2 suppression impairs the developmental potential of embryonic stem cells. *Nature* **548**, 219-223, doi:10.1038/nature23274 (2017).

53 Parchem, R. J. *et al.* Two miRNA clusters reveal alternative paths in late-stage reprogramming. *Cell Stem Cell* **14**, 617-631, doi:10.1016/j.stem.2014.01.021 (2014).

54 Zhang, J. *et al.* LIN28 Regulates Stem Cell Metabolism and Conversion to Primed Pluripotency. *Cell Stem Cell* **19**, 66-80, doi:10.1016/j.stem.2016.05.009 (2016).

55 Fidalgo, M. *et al.* Zfp281 Coordinates Opposing Functions of Tet1 and Tet2 in Pluripotent States. *Cell Stem Cell* **19**, 355-369, doi:10.1016/j.stem.2016.05.025 (2016).

56 Luo, Z. *et al.* Zic2 is an enhancer-binding factor required for embryonic stem cell specification. *Mol Cell* **57**, 685-694, doi:10.1016/j.molcel.2015.01.007 (2015).

57 Betschinger, J. *et al.* Exit from pluripotency is gated by intracellular redistribution of the bHLH transcription factor Tfe3. *Cell* **153**, 335-347, doi:10.1016/j.cell.2013.03.012 (2013).

58 Brandenberger, R. *et al.* Transcriptome characterization elucidates signaling networks that control human ES cell growth and differentiation. *Nat Biotechnol* **22**, 707-716, doi:10.1038/nbt971 (2004).

59 Wang, Z. X. *et al.* The transcription factor Zfp281 controls embryonic stem cell pluripotency by direct activation and repression of target genes. *Stem Cells* **26**, 2791-2799, doi:10.1634/stemcells.2008-0443 (2008).

60 Mayer, D. *et al.* Zfp281 orchestrates interconversion of pluripotent states by engaging Ehmt1 and Zic2. *EMBO J* **39**, e102591, doi:10.15252/embj.2019102591 (2020).

61 Okuda, A. *et al.* UTF1, a novel transcriptional coactivator expressed in pluripotent embryonic stem cells and extra-embryonic cells. *EMBO J* **17**, 2019-2032, doi:10.1093/emboj/17.7.2019 (1998).

62 Kooistra, S. M., Thummer, R. P. & Eggen, B. J. Characterization of human UTF1, a chromatin-associated protein with repressor activity expressed in pluripotent cells. *Stem Cell Res* **2**, 211-218, doi:10.1016/j.scr.2009.02.001 (2009).

63 Jia, J. *et al.* Regulation of pluripotency and self- renewal of ESCs through epigenetic-threshold modulation and mRNA pruning. *Cell* **151**, 576-589, doi:10.1016/j.cell.2012.09.023 (2012).

64 Respuela, P. *et al.* Foxd3 Promotes Exit from Naive Pluripotency through Enhancer Decommissioning and Inhibits Germline Specification. *Cell Stem Cell* **18**, 118-133, doi:10.1016/j.stem.2015.09.010 (2016).

65 Yasunaga, M. *et al.* Induction and monitoring of definitive and visceral endoderm differentiation of mouse ES cells. *Nat Biotechnol* **23**, 1542-1550, doi:10.1038/nbt1167 (2005).

66 Engert, S. *et al.* Wnt/beta-catenin signalling regulates Sox17 expression and is essential for organizer and endoderm formation in the mouse. *Development* **140**, 3128-3138, doi:10.1242/dev.088765 (2013).

67 Tosic, J. *et al.* Eomes and Brachyury control pluripotency exit and germ-layer segregation by changing the chromatin state. *Nat Cell Biol* **21**, 1518-1531, doi:10.1038/s41556-019-0423-1 (2019).

68 Ying, Q. L., Stavridis, M., Griffiths, D., Li, M. & Smith, A. Conversion of embryonic stem cells into neuroectodermal precursors in adherent monoculture. *Nat Biotechnol* **21**, 183-186, doi:10.1038/nbt780 (2003).

69 Langfelder, P. & Horvath, S. WGCNA: an R package for weighted correlation network analysis. *BMC Bioinformatics* **9**, 559, doi:10.1186/1471-2105-9-559 (2008).

70 Ogawa, K., Nishinakamura, R., Iwamatsu, Y., Shimosato, D. & Niwa, H. Synergistic action of Wnt and LIF in maintaining pluripotency of mouse ES cells. *Biochem Biophys Res Commun* **343**, 159-166, doi:10.1016/j.bbrc.2006.02.127 (2006).

71 Hao, J., Li, T. G., Qi, X., Zhao, D. F. & Zhao, G. Q. WNT/beta-catenin pathway up-regulates Stat3 and converges on LIF to prevent differentiation of mouse embryonic stem cells. *Dev Biol* **290**, 81-91, doi:10.1016/j.ydbio.2005.11.011 (2006).

72 Singla, D. K., Schneider, D. J., LeWinter, M. M. & Sobel, B. E. wnt3a but not wnt11 supports self-renewal of embryonic stem cells. *Biochem Biophys Res Commun* **345**, 789-795, doi:10.1016/j.bbrc.2006.04.125 (2006).

73 Takao, Y., Yokota, T. & Koide, H. Beta-catenin up-regulates Nanog expression through interaction with Oct-3/4 in embryonic stem cells. *Biochem Biophys Res Commun* **353**, 699-705, doi:10.1016/j.bbrc.2006.12.072 (2007).

74 Tsukiyama, T. & Ohinata, Y. A modified EpiSC culture condition containing a GSK3 inhibitor can support germline-competent pluripotency in mice. *PLoS One* **9**, e95329, doi:10.1371/journal.pone.0095329 (2014).

75 Sugimoto, M. *et al.* A simple and robust method for establishing homogeneous mouse epiblast stem cell lines by wnt inhibition. *Stem Cell Reports* **4**, 744-757, doi:10.1016/j.stemcr.2015.02.014 (2015).

76 Sumi, T., Oki, S., Kitajima, K. & Meno, C. Epiblast ground state is controlled by canonical Wnt/beta-catenin signaling in the postimplantation mouse embryo and epiblast stem cells. *PLoS One* **8**, e63378, doi:10.1371/journal.pone.0063378 (2013).

77 Liu, K., Sun, Y., Liu, D. & Ye, S. Inhibition of Wnt/beta-catenin signaling by IWR1 induces expression of Foxd3 to promote mouse epiblast stem cell self-renewal. *Biochem Biophys Res Commun* **490**, 616-622, doi:10.1016/j.bbrc.2017.06.086 (2017).

78 Osteil, P. *et al.* Dynamics of Wnt activity on the acquisition of ectoderm potency in epiblast stem cells. *Development* **146**, doi:10.1242/dev.172858 (2019).

79 Kurek, D. *et al.* Endogenous WNT signals mediate BMP-induced and spontaneous differentiation of epiblast stem cells and human embryonic stem cells. *Stem Cell Reports* **4**, 114-128, doi:10.1016/j.stemcr.2014.11.007 (2015).

80 Dobin, A. *et al.* STAR: ultrafast universal RNA-seq aligner. *Bioinformatics* **29**, 15-21, doi:10.1093/bioinformatics/bts635 (2013).

81 Anders, S., Pyl, P. T. & Huber, W. HTSeq--a Python framework to work with high-throughput sequencing data. *Bioinformatics* **31**, 166-169, doi:10.1093/bioinformatics/btu638 (2015).

82 Robinson, M. D., McCarthy, D. J. & Smyth, G. K. edgeR: a Bioconductor package for differential expression analysis of digital gene expression data. *Bioinformatics* **26**, 139-140, doi:10.1093/bioinformatics/btp616 (2010).

83 Yip, A. M. & Horvath, S. Gene network interconnectedness and the generalized topological overlap measure. *BMC Bioinformatics* **8**, 22, doi:10.1186/1471-2105-8-22 (2007).

84 Langfelder, P., Zhang, B. & Horvath, S. Defining clusters from a hierarchical cluster tree: the Dynamic Tree Cut package for R. *Bioinformatics* **24**, 719-720, doi:10.1093/bioinformatics/btm563 (2008).

85 Hubert, L., Arabie, P. . Comparing partitions. *Journal of Classification* **2**, 193-218, doi:10.1007/BF01908075 (1985).

86 Ashburner, M. *et al.* Gene ontology: tool for the unification of biology. The Gene Ontology Consortium. *Nat Genet* **25**, 25-29, doi:10.1038/75556 (2000).

87 Kanehisa, M. & Goto, S. KEGG: kyoto encyclopedia of genes and genomes. *Nucleic Acids Res* **28**, 27-30, doi:10.1093/nar/28.1.27 (2000).

88 Yu, G., Wang, L. G., Han, Y. & He, Q. Y. clusterProfiler: an R package for comparing biological themes among gene clusters. *OMICS* **16**, 284-287, doi:10.1089/omi.2011.0118 (2012).

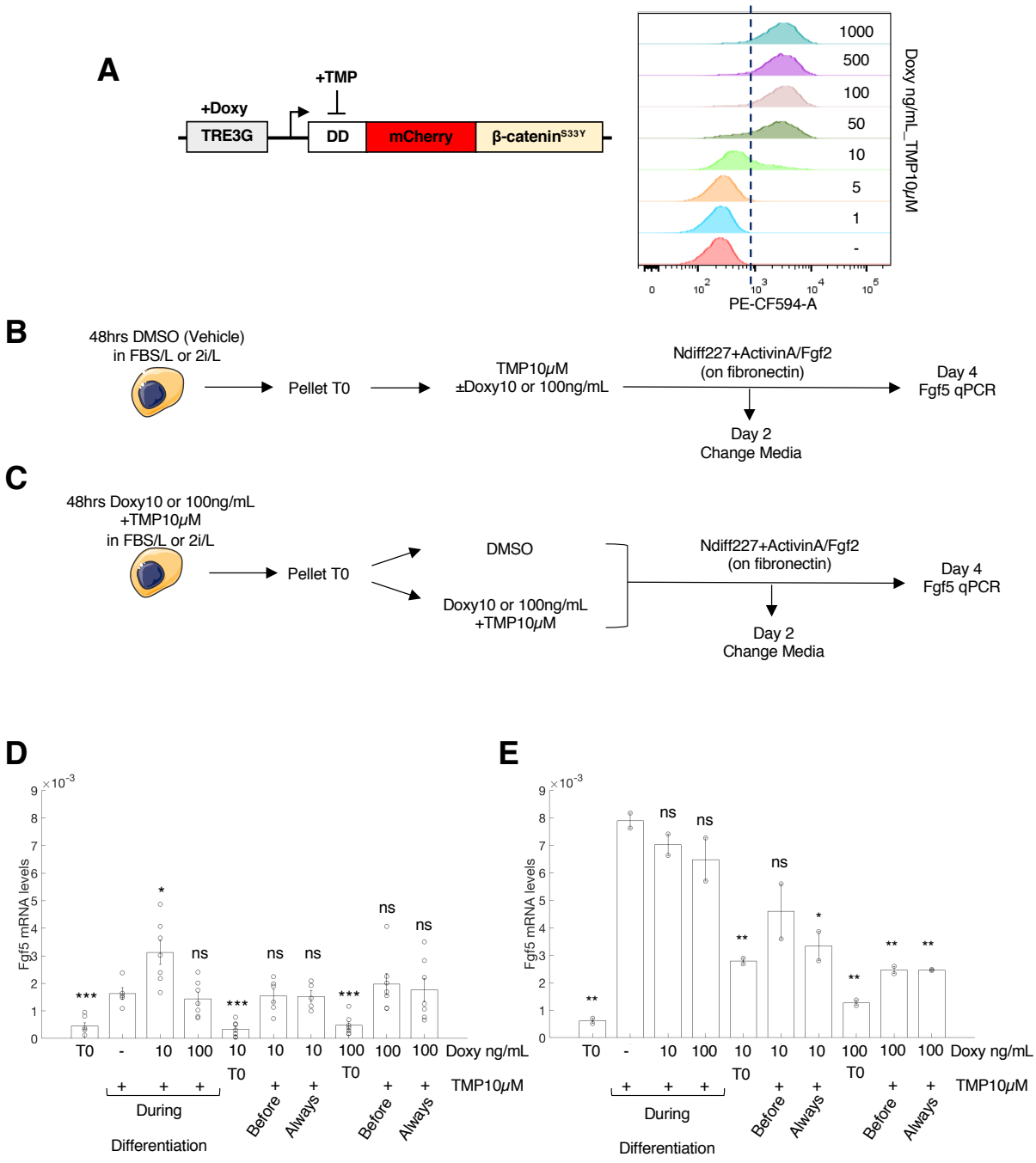
A
+Doxy
+TMP
TRE3G
DD
mCherry
β-catenin S33Y
1000
500
100
50
10
5
1
-
Doxy ng/mL_TMP10μM
PE-CF594-A
B
48hrs DMSO (Vehicle)
in FBS/L or 2i/L
Pellet T0
TMP10μM
±Doxy10 or 100ng/mL
Ndiff227+ActivinA/Fgf2
(on fibronectin)
Day 4
Fgf5 qPCR
Day 2
Change Media
C
48hrs Doxy10 or 100ng/mL
+TMP10μM
in FBS/L or 2i/L
Pellet T0
DMSO
Doxy10 or 100ng/mL
+TMP10μM
Ndiff227+ActivinA/Fgf2
(on fibronectin)
Day 4
Fgf5 qPCR
Day 2
Change Media
D
Fgf5 mRNA levels
Doxy ng/mL
TMP10μM
During
Differentiation
Before
Always
E
Fgf5 mRNA levels
Doxy ng/mL
TMP10μM
During
Differentiation
Before
Always

Figure1

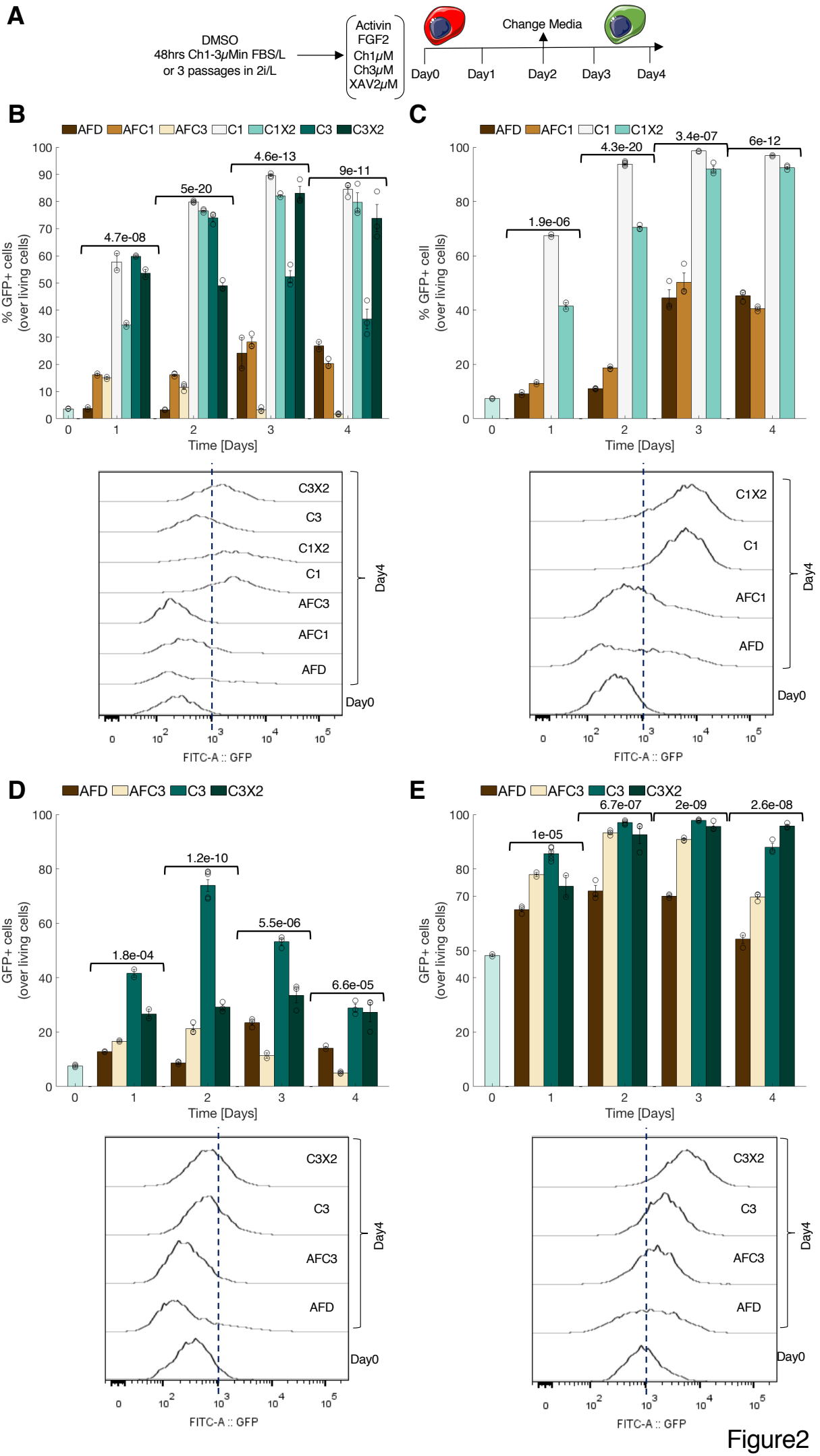
A
DMSO
48hrs Ch1-3μMin FBS/L
or 3 passages in 2i/L
Activin
FGF2
Ch1μM
Ch3μM
XAV2μM
Change Media
Day0
Day1
Day2
Day3
Day4
B
AFD AFC1 AFC3 C1 C1X2 C3 C3X2
% GFP+ cells
(over living cells)
4.7e-08
5e-20
4.6e-13
9e-11
Time [Days]
C3X2
C3
C1X2
C1
AFC3
AFC1
AFD
Day4
Day0
FITC-A :: GFP
C
AFD AFC1 C1 C1X2
% GFP+ cell
(over living cells)
1.9e-06
4.3e-20
3.4e-07
6e-12
Time [Days]
C1X2
C1
AFC1
AFD
Day4
Day0
FITC-A :: GFP
D
AFD AFC3 C3 C3X2
GFP+ cells
(over living cells)
1.8e-04
1.2e-10
5.5e-06
6.6e-05
Time [Days]
C3X2
C3
AFC3
AFD
Day4
Day0
FITC-A :: GFP
E
AFD AFC3 C3 C3X2
GFP+ cells
(over living cells)
1e-05
6.7e-07
2e-09
2.6e-08
Time [Days]
C3X2
C3
AFC3
AFD
Day4
Day0
FITC-A :: GFP

Figure2

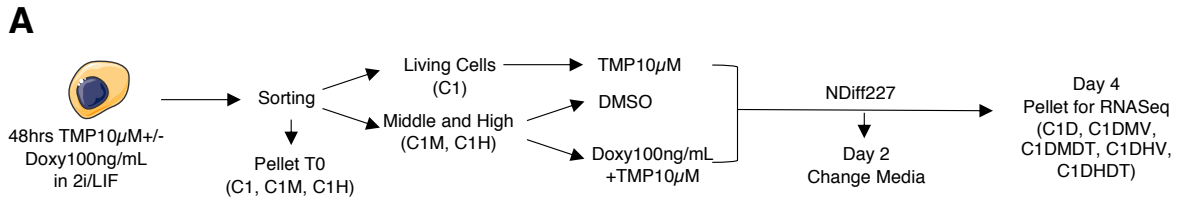
A
48hrs TMP10μM+/-
Doxy100ng/mL
in 2i/LIF
Sorting
Pellet T0
(C1, C1M, C1H)
Living Cells
(C1)
Middle and High
(C1M, C1H)
TMP10μM
DMSO
Doxy100ng/mL
+TMP10μM
NDiff227
Day 2
Change Media
Day 4
Pellet for RNASeq
(C1D, C1DMV,
C1DMDT, C1DHV,
C1DHDT)

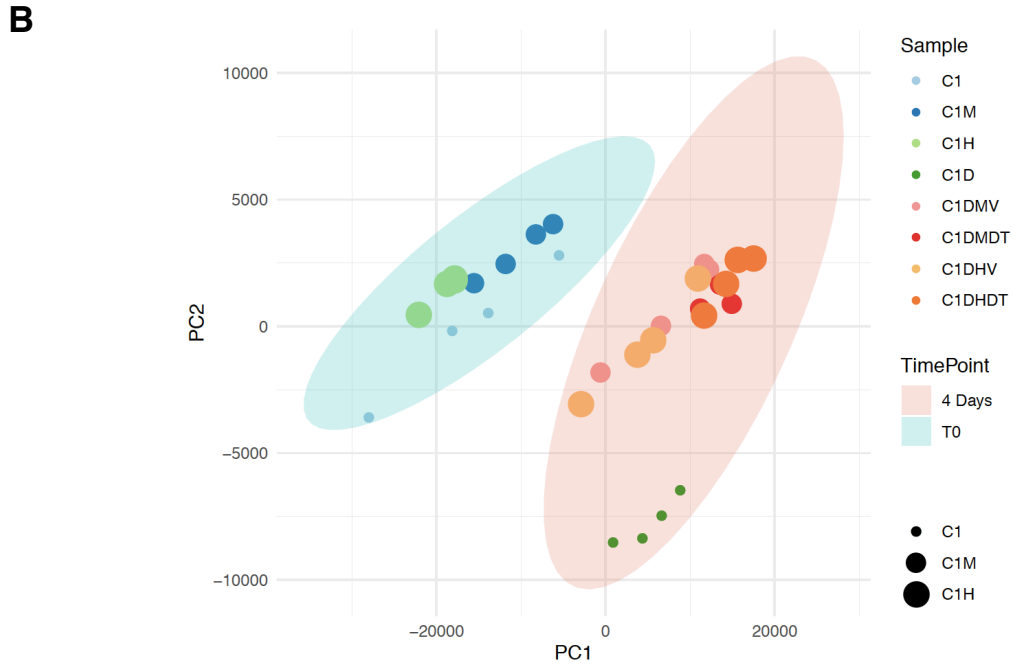
B
Sample
C1
C1M
C1H
C1D
C1DMV
C1DMDT
C1DHV
C1DHDT
TimePoint
4 Days
T0
C1
C1M
C1H
PC2
PC1
10000
5000
0
−5000
−10000
−20000
0
20000

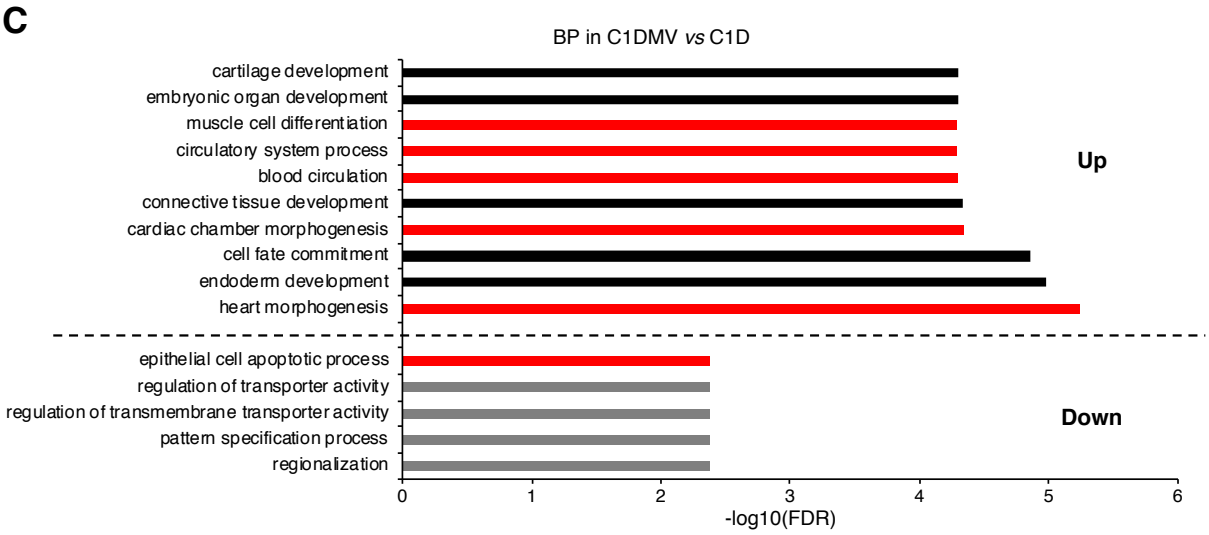
C
BP in C1DMV vs C1D
cartilage development
embryonic organ development
muscle cell differentiation
circulatory system process
blood circulation
connective tissue development
cardiac chamber morphogenesis
cell fate commitment
endoderm development
heart morphogenesis
Up
epithelial cell apoptotic process
regulation of transporter activity
regulation of transmembrane transporter activity
pattern specification process
regionalization
Down
0
1
2
3
4
5
6
-log10(FDR)

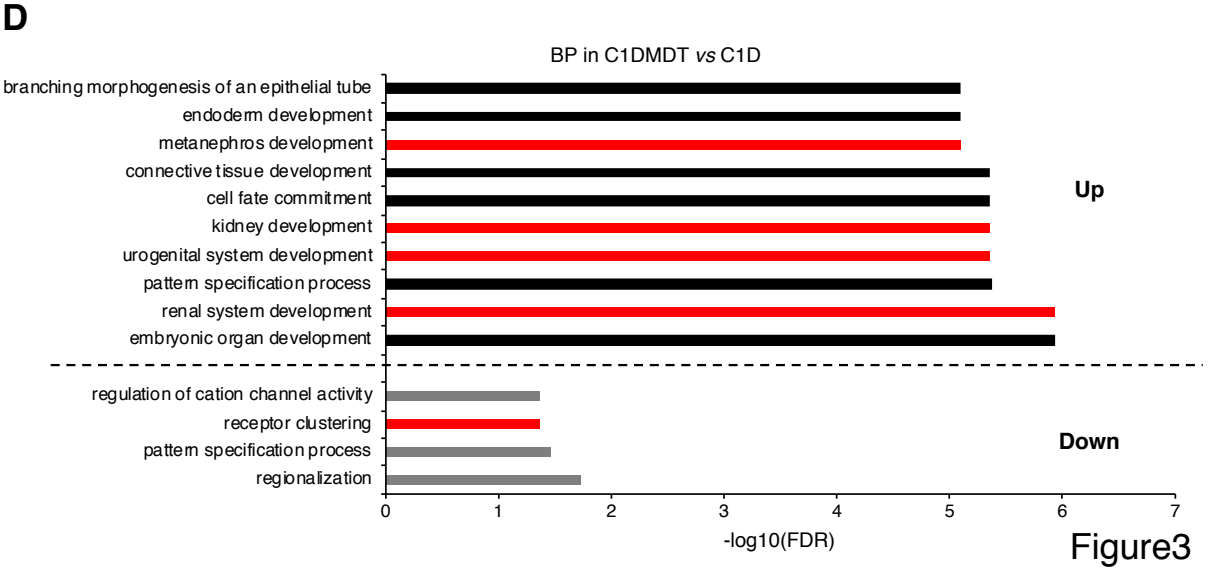
D
BP in C1DMDT vs C1D
branching morphogenesis of an epithelial tube
endoderm development
metanephros development
connective tissue development
cell fate commitment
kidney development
urogenital system development
pattern specification process
renal system development
embryonic organ development
Up
regulation of cation channel activity
receptor clustering
pattern specification process
regionalization
Down
0
1
2
3
4
5
6
7
-log10(FDR)

Figure3

E

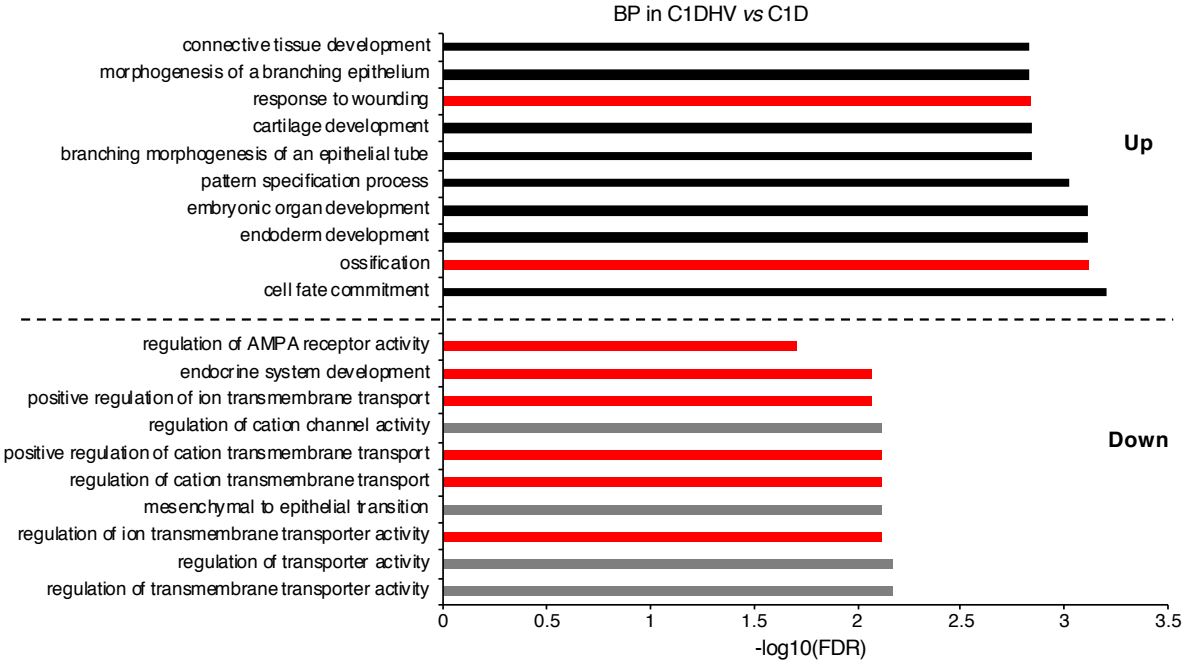
BP in C1DHV *vs* C1D
connective tissue development
morphogenesis of a branching epithelium
response to wounding
cartilage development
branching morphogenesis of an epithelial tube
pattern specification process
embryonic organ development
endoderm development
ossification
cell fate commitment
Up
regulation of AMPA receptor activity
endocrine system development
positive regulation of ion transmembrane transport
regulation of cation channel activity
positive regulation of cation transmembrane transport
regulation of cation transmembrane transport
mesenchymal to epithelial transition
regulation of ion transmembrane transporter activity
regulation of transporter activity
regulation of transmembrane transporter activity
Down
0
0.5
1
1.5
2
2.5
3
3.5
-log10(FDR)

F

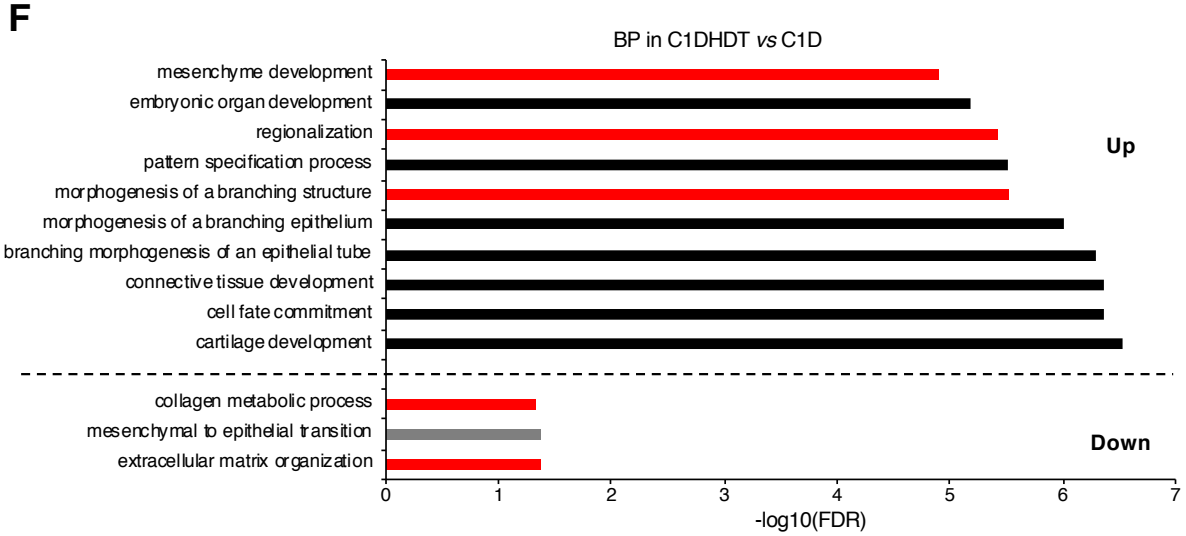
BP in C1DHDT *vs* C1D
mesenchyme development
embryonic organ development
regionalization
pattern specification process
morphogenesis of a branching structure
morphogenesis of a branching epithelium
branching morphogenesis of an epithelial tube
connective tissue development
cell fate commitment
cartilage development
Up
collagen metabolic process
mesenchymal to epithelial transition
extracellular matrix organization
Down
0
1
2
3
4
5
6
7
-log10(FDR)

Figure3

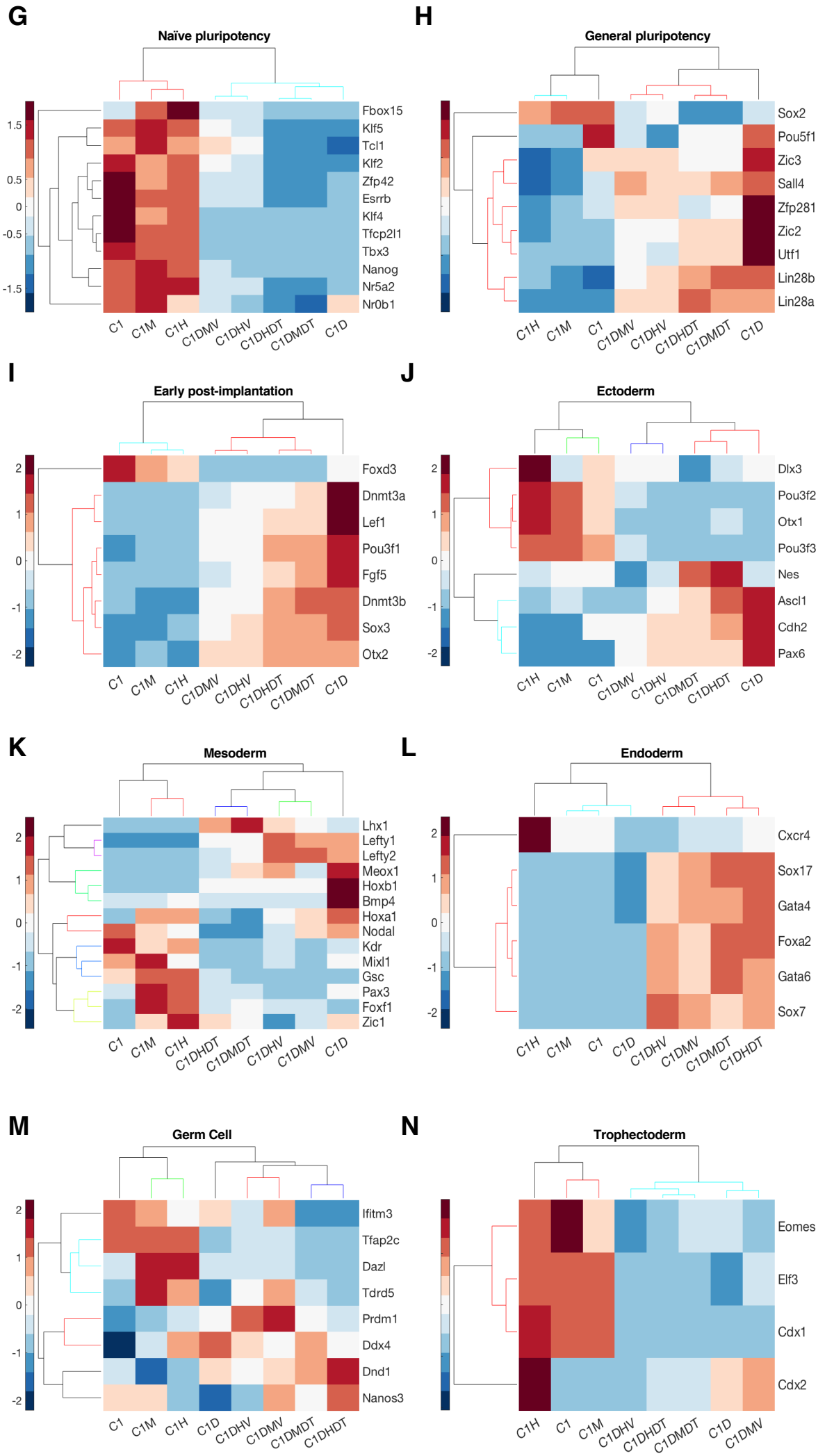
G
Naïve pluripotency
Fbox15
Klf5
Tcl1
Klf2
Zfp42
Esrrb
Klf4
Tfcp2l1
Tbx3
Nanog
Nr5a2
Nr0b1
C1 C1M C1H C1DMV C1DHV C1DHDT C1DMDT C1D
H
General pluripotency
Sox2
Pou5f1
Zic3
Sall4
Zfp281
Zic2
Utf1
Lin28b
Lin28a
C1H C1M C1 C1DMV C1DHV C1DHDT C1DMDT C1D
I
Early post-implantation
Foxd3
Dnmt3a
Lef1
Pou3f1
Fgf5
Dnmt3b
Sox3
Otx2
C1 C1M C1H C1DMV C1DHV C1DHDT C1DMDT C1D
J
Ectoderm
Dlx3
Pou3f2
Otx1
Pou3f3
Nes
Ascl1
Cdh2
Pax6
C1H C1M C1 C1DMV C1DHV C1DMDT C1DHDT C1D
K
Mesoderm
Lhx1
Lefty1
Lefty2
Meox1
Hoxb1
Bmp4
Hoxa1
Nodal
Kdr
Mixl1
Gsc
Pax3
Foxf1
Zic1
C1 C1M C1H C1DHDT C1DMDT C1DHV C1DMV C1D
L
Endoderm
Cxcr4
Sox17
Gata4
Foxa2
Gata6
Sox7
C1H C1M C1 C1D C1DHV C1DMV C1DMDT C1DHDT
M
Germ Cell
Ifitm3
Tfap2c
Dazl
Tdrd5
Prdm1
Ddx4
Dnd1
Nanos3
C1 C1M C1H C1D C1DHV C1DMV C1DMDT C1DHDT
N
Trophectoderm
Eomes
Elf3
Cdx1
Cdx2
C1H C1 C1M C1DHV C1DHDT C1DMDT C1D C1DMV

Figure3

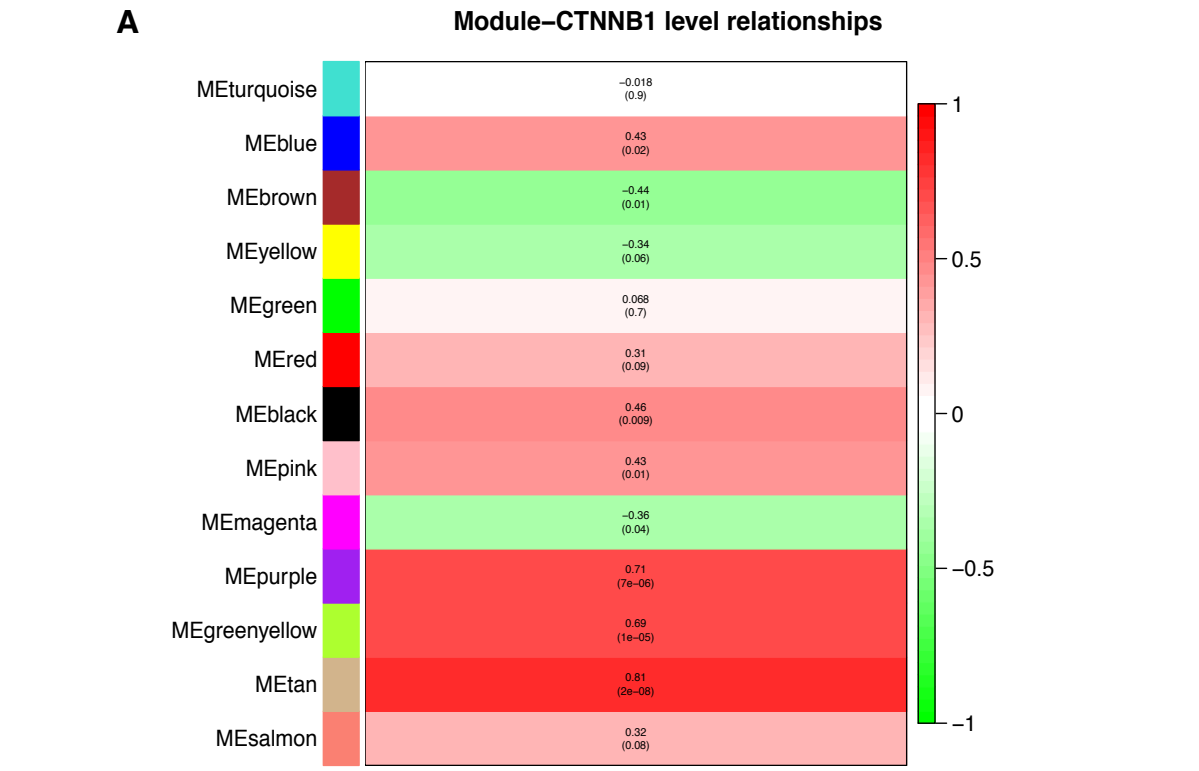
A
Module–CTNNB1 level relationships
MEturquoise
MEblue
MEbrown
MEyellow
MEgreen
MEred
MEblack
MEpink
MEmagenta
MEpurple
MEgreenyellow
MEtan
MEsalmon
−0.018
(0.9)
0.43
(0.02)
−0.44
(0.01)
−0.34
(0.06)
0.068
(0.7)
0.31
(0.09)
0.46
(0.009)
0.43
(0.01)
−0.36
(0.04)
0.71
(7e−06)
0.69
(1e−05)
0.81
(2e−08)
0.32
(0.08)
1
0.5
0
−0.5
−1

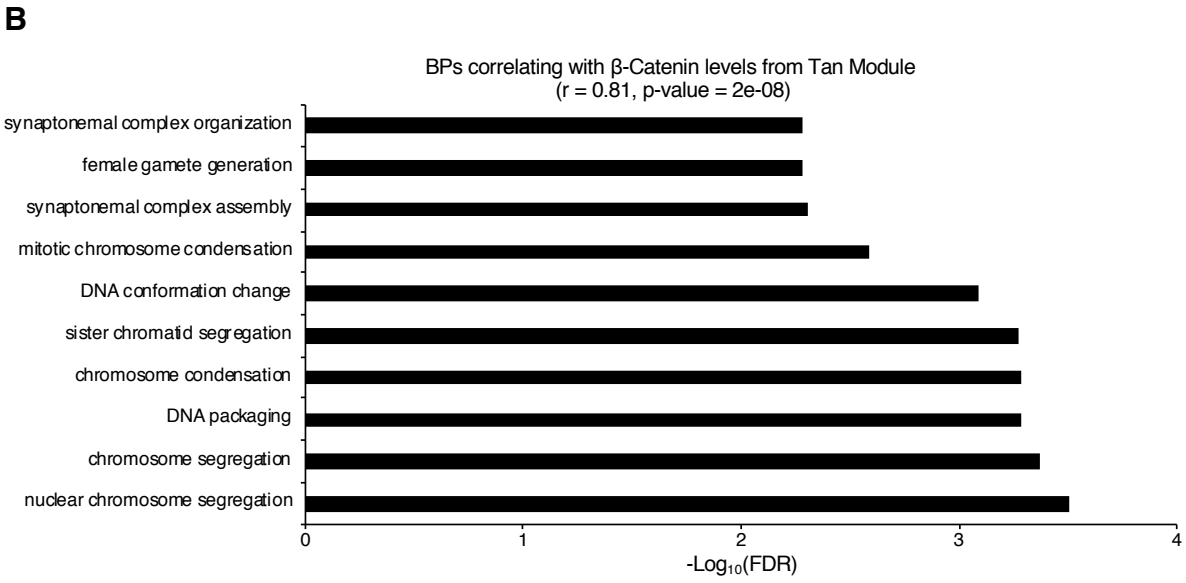
B
BPs correlating with β-Catenin levels from Tan Module
(r = 0.81, p-value = 2e-08)
synaptonemal complex organization
female gamete generation
synaptonemal complex assembly
mitotic chromosome condensation
DNA conformation change
sister chromatid segregation
chromosome condensation
DNA packaging
chromosome segregation
nuclear chromosome segregation
0
1
2
3
4
-Log10(FDR)

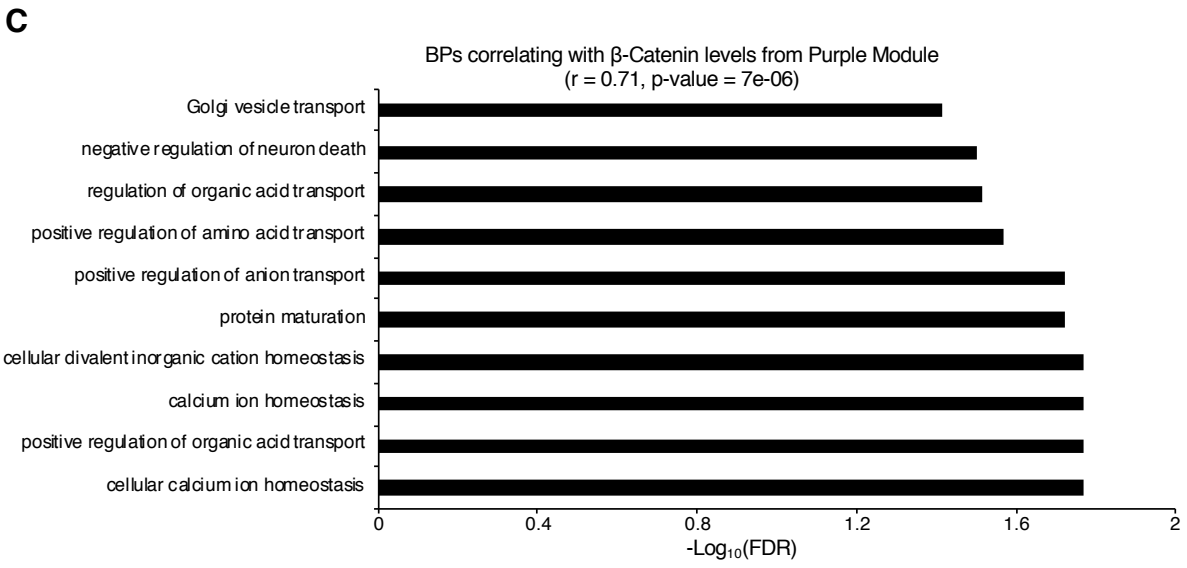
C
BPs correlating with β-Catenin levels from Purple Module
(r = 0.71, p-value = 7e-06)
Golgi vesicle transport
negative regulation of neuron death
regulation of organic acid transport
positive regulation of amino acid transport
positive regulation of anion transport
protein maturation
cellular divalent inorganic cation homeostasis
calcium ion homeostasis
positive regulation of organic acid transport
cellular calcium ion homeostasis
0
0.4
0.8
1.2
1.6
2
-Log10(FDR)

Figure4

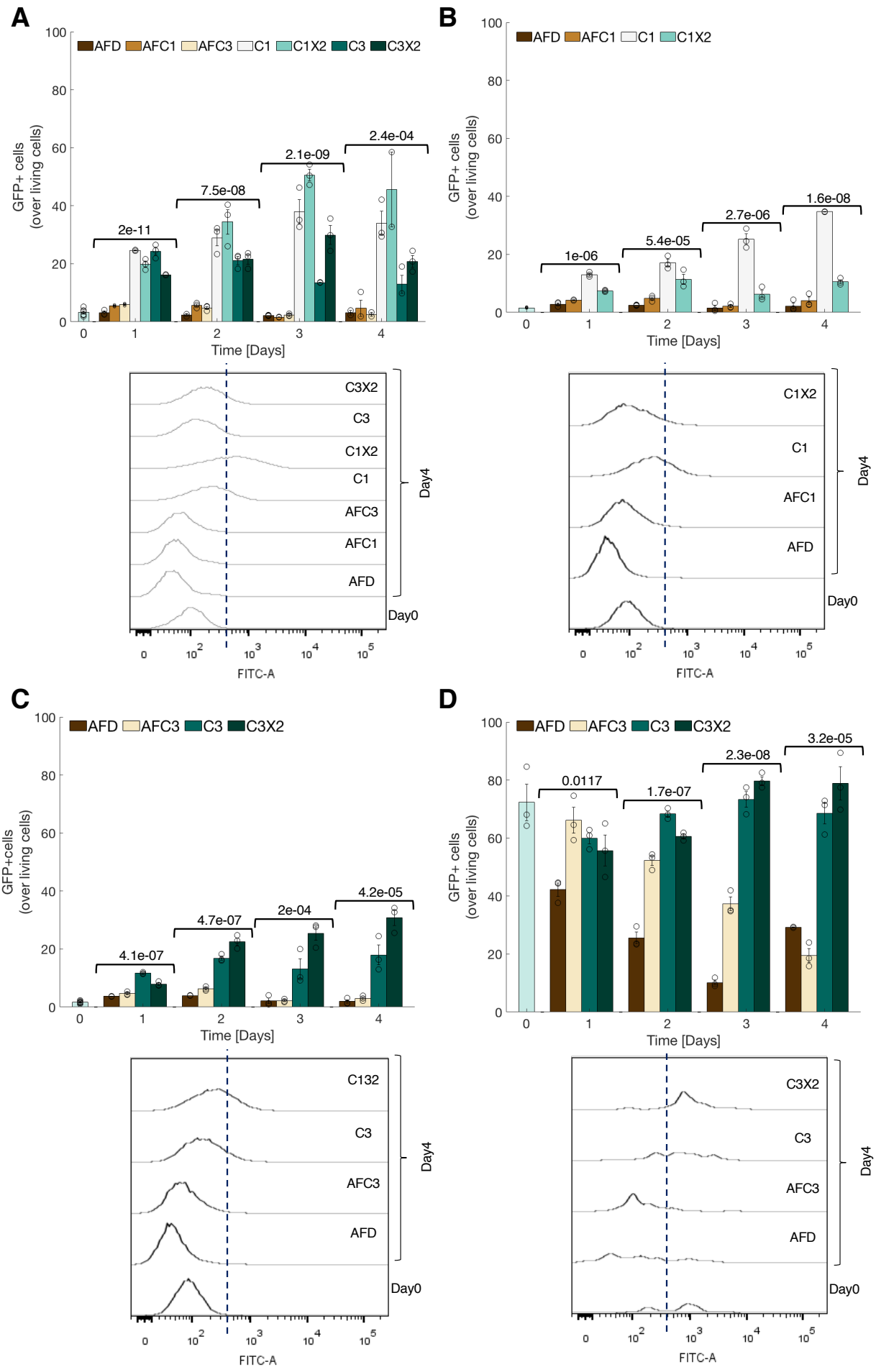

Supplementary Figure2

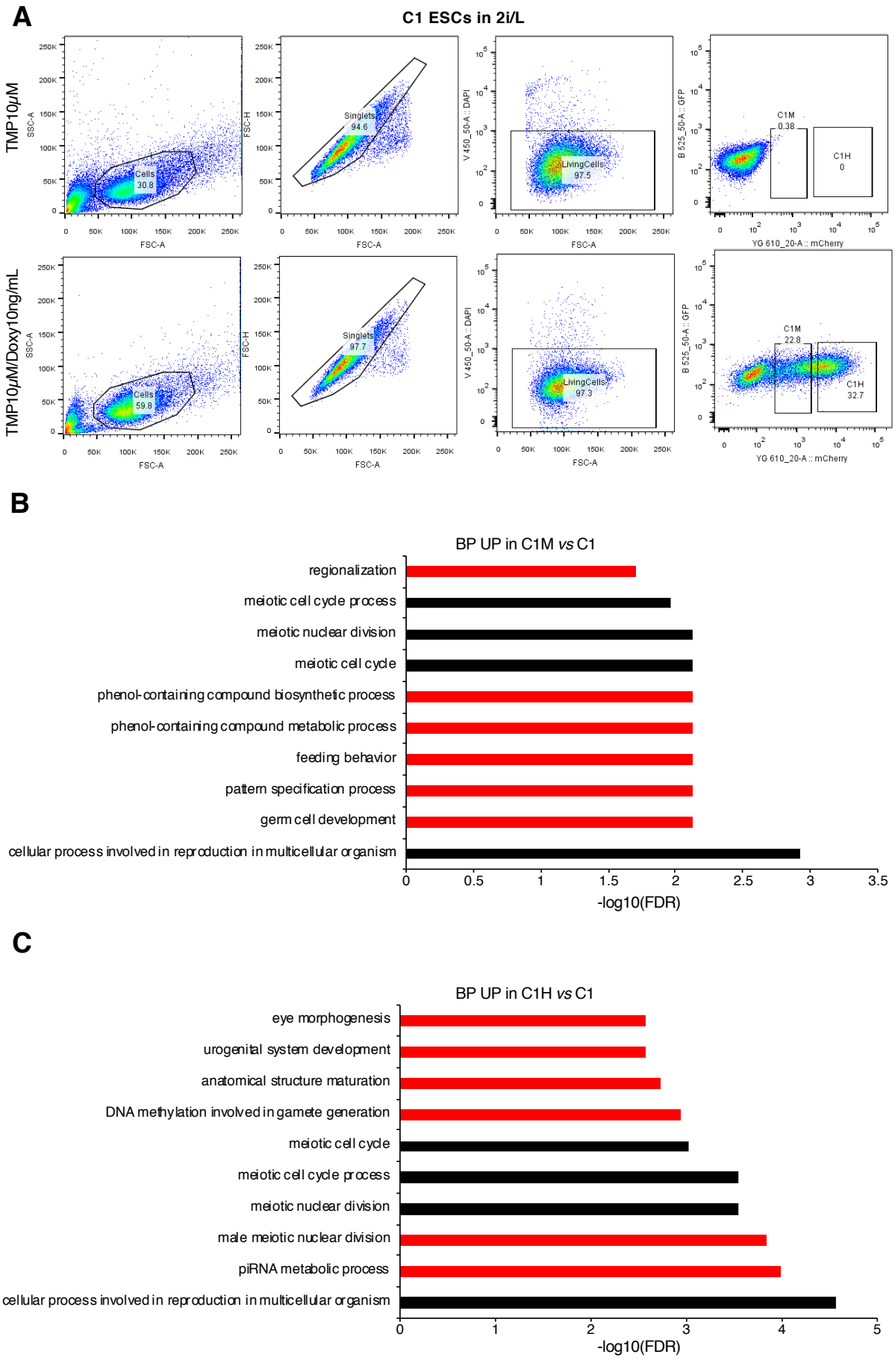

Supplementary Figure3

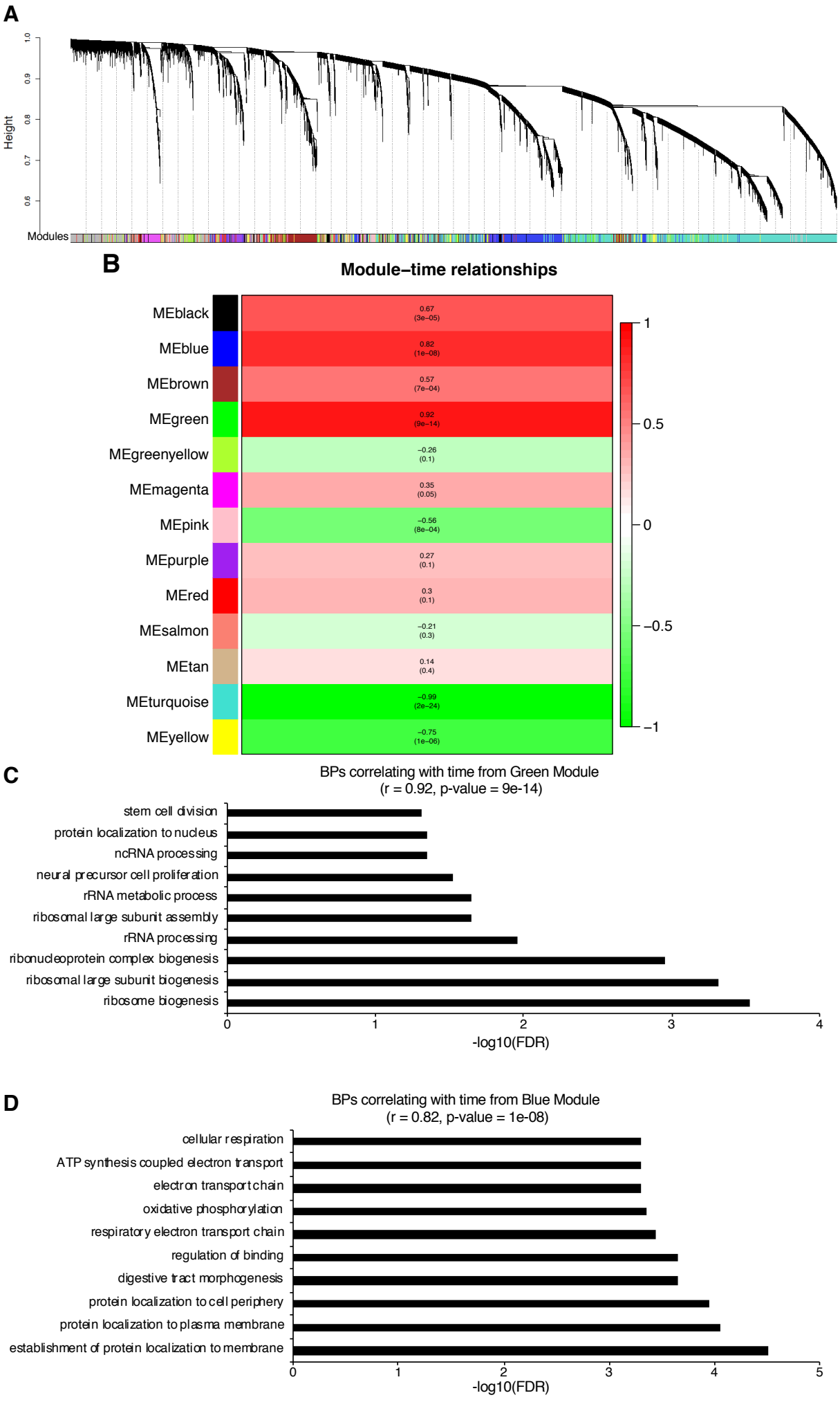

Supplementary Figure4

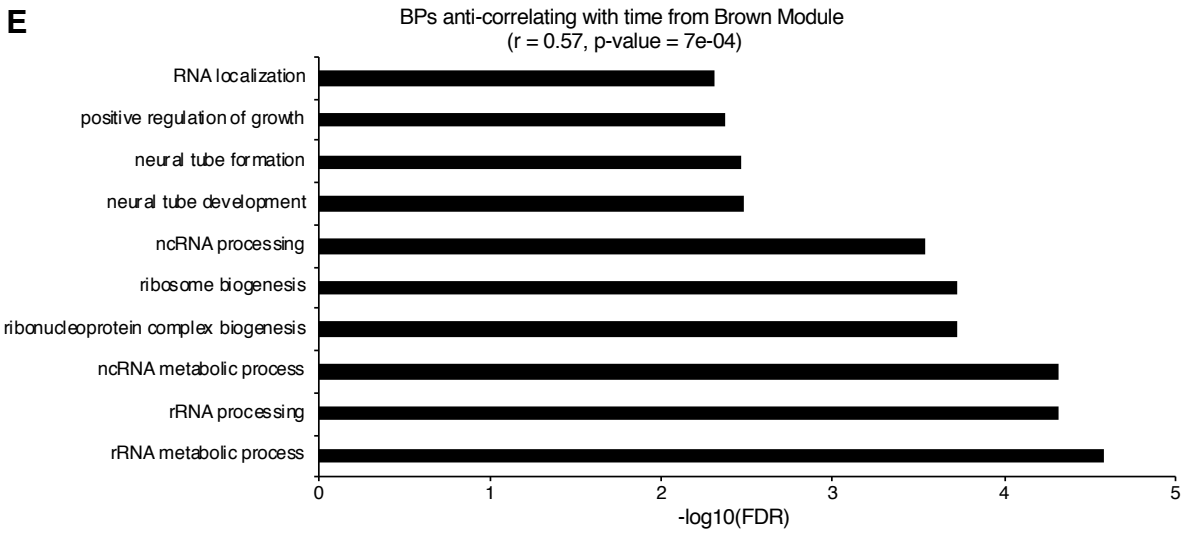

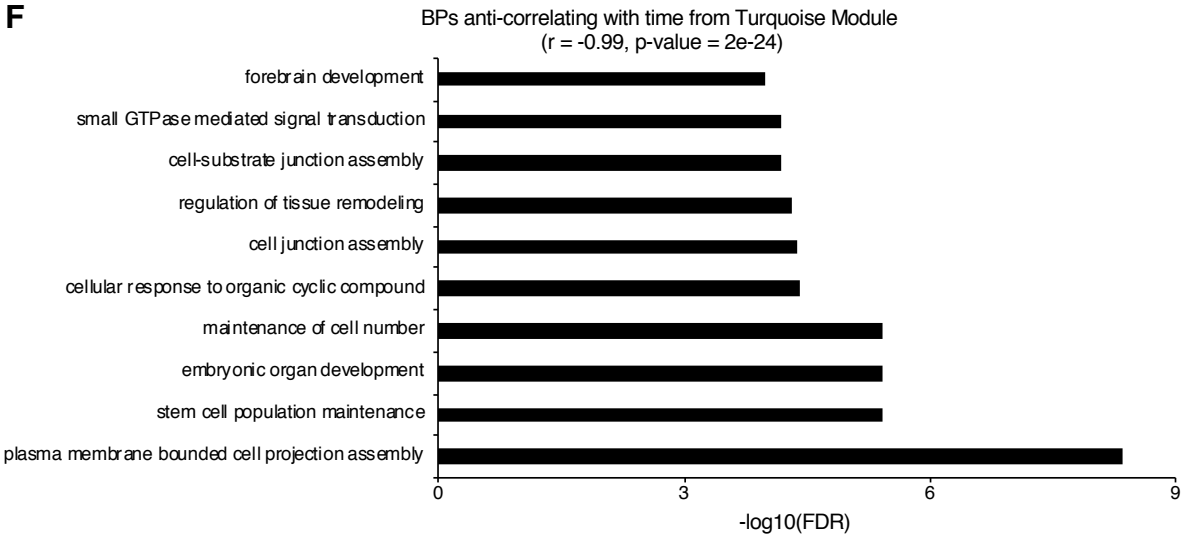

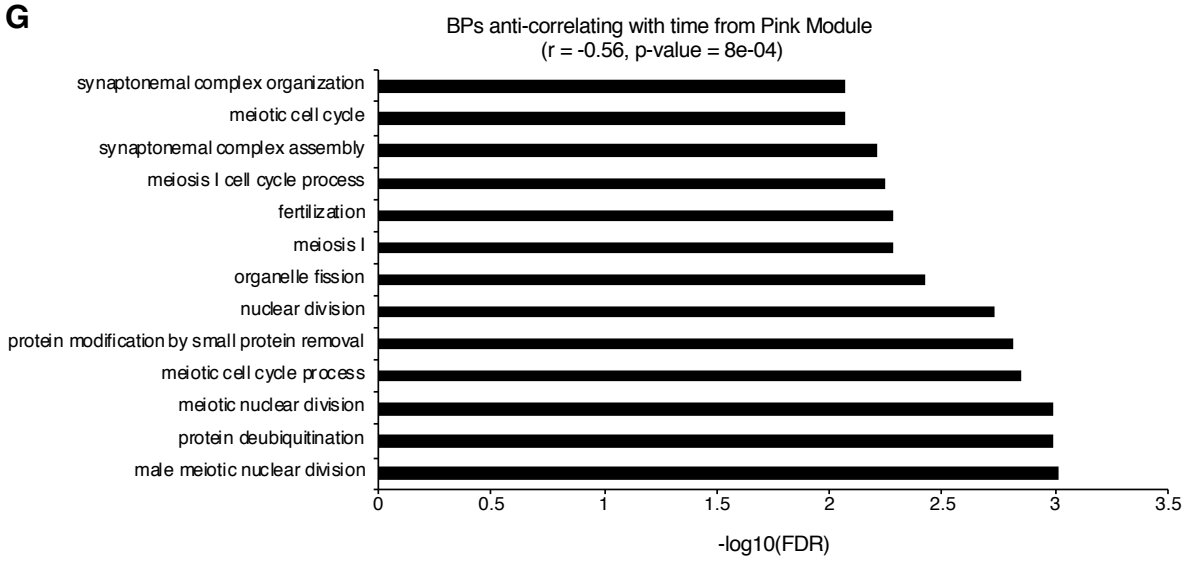

Supplementary Figure4